Earth Syst. Sci. Data, 13, 5689–5710, 2021
https://doi.org/10.5194/essd-13-5689-2021

Open Access Earth System Science Data

Landsat-based Irrigation Dataset (LANID): 30 m resolution maps of irrigation distribution, frequency, and change for the US, 1997–2017

Yanhua Xie[1,2], **Holly K. Gibbs**[1,2,3], **and Tyler J. Lark**[1,2]

[1]Nelson Institute Center for Sustainability and the Global Environment (SAGE), University of Wisconsin-Madison, Madison, 53726, USA
[2]DOE Great Lakes Bioenergy Research Center, University of Wisconsin-Madison, Madison, 53726, USA
[3]Department of Geography, University of Wisconsin-Madison, Madison, 53706, USA

Correspondence: Yanhua Xie (xie78@wisc.edu)

Received: 22 June 2021 – Discussion started: 30 June 2021
Revised: 5 October 2021 – Accepted: 25 October 2021 – Published: 8 December 2021

Abstract. Data on irrigation patterns and trends at field-level detail across broad extents are vital for assessing and managing limited water resources. Until recently, there has been a scarcity of comprehensive, consistent, and frequent irrigation maps for the US. Here we present the new Landsat-based Irrigation Dataset (LANID), which is comprised of 30 m resolution annual irrigation maps covering the conterminous US (CONUS) for the period of 1997–2017. The main dataset identifies the annual extent of irrigated croplands, pastureland, and hay for each year in the study period. Derivative maps include layers on maximum irrigated extent, irrigation frequency and trends, and identification of formerly irrigated areas and intermittently irrigated lands. Temporal analysis reveals that 38.5×10^6 ha of croplands and pasture–hay has been irrigated, among which the yearly active area ranged from ~ 22.6 to 24.7×10^6 ha. The LANID products provide several improvements over other irrigation data including field-level details on irrigation change and frequency, an annual time step, and a collection of $\sim 10\,000$ visually interpreted ground reference locations for the eastern US where such data have been lacking. Our maps demonstrated overall accuracy above 90 % across all years and regions, including in the more humid and challenging-to-map eastern US, marking a significant advancement over other products, whose accuracies ranged from 50 % to 80 %. In terms of change detection, our maps yield per-pixel transition accuracy of 81 % and show good agreement with US Department of Agriculture reports at both county and state levels. The described annual maps, derivative layers, and ground reference data provide users with unique opportunities to study local to nationwide trends, driving forces, and consequences of irrigation and encourage the further development and assessment of new approaches for improved mapping of irrigation, especially in challenging areas like the eastern US. The annual LANID maps, derivative products, and ground reference data are available through https://doi.org/10.5281/zenodo.5548555 (Xie and Lark, 2021a).

1 Introduction

Irrigated agriculture is vital to global food security. Irrigation helps stabilize farm production by enhancing land productivity that would otherwise be lower due to water limitations to plant growth. In the US, approximately 14.6 % of the total cropland is irrigated (USDA-NASS, 2019). Despite this relatively small proportion, irrigated agriculture plays a significantly disproportionate role in agriculture, accounting for major proportions of the economic value and environmental impacts; irrigated farms account for 54 % of the total value of crop sales (USDA-NASS, 2021). However, agricultural irrigation uses over 40 % of total freshwater withdrawals and 80 % to 90 % of consumptive water use in the US (Dieter et al., 2018; USDA, 2021). As a result, improved management and understanding of irrigation use and trends offer a

key leverage point to improve the sustainability of US agriculture.

Knowledge of the spatial and temporal patterns of irrigation is a crucial first step to improve this understanding and management and to help policymakers make decisions to support sustainable water use for crop production. However, the spatiotemporal patterns of irrigation and their impacts are not well understood, even for data-rich countries like the US. This insufficient knowledge about irrigation hampers a much larger body of research and applications, such as the modeling of land surface characteristics, climate and weather, and the growth of crops and other vegetation. For those applications that do incorporate irrigation modules, they are typically based on infrequently updated coarse-resolution global maps that cannot represent the precise locations of irrigated fields (Zaussinger et al., 2019; Ozdogan et al., 2010). As such, there is significant need for field-relevant resolution maps of irrigated agricultural land and its temporal changes. The value of such detailed irrigation information is further magnified as society formulates strategies towards sustainable use of limited water resources from local to global scales under the context of increasing food and fuel demands, climate change and extremes, and population growth (Lark et al., 2015; Rosegrant et al., 2009; Seto et al., 2012; Seager et al., 2012; Mcdonald et al., 2011).

Despite the growing importance of field-level irrigation information to a wide array of research questions and applications, currently available irrigation maps that cover the entire or part of the conterminous US (CONUS) suffer from limitations related to spatial resolution, update frequency, geographical coverage, and mapping accuracy (Table 1). For example, the spatial resolution of all nationwide maps (except for LANID-US 2012) ranges from 250 m to kilometers, which is problematic for many local applications that require accurate field characterization (Wardlow and Callahan, 2014; Deines et al., 2017; Ozdogan and Gutman, 2008; Xie et al., 2019b; Brown and Pervez, 2014). Just as importantly, all these nationwide irrigation maps are infrequently updated and mapped at either a single date or at intervals of 5 years to decades (e.g., Shrestha et al., 2021; Brown and Pervez, 2014; Ozdogan and Gutman, 2008). Due to annual crop rotations, fallow practices, and climate variation, however, irrigation use and decision making are extremely dynamic. Accordingly, more timely information is needed to understand changes in irrigation and the associated impacts including water use and availability.

Recent years have witnessed unprecedented development of land use/cover mapping owing to the increasing availability of high- to moderate-resolution remote sensing data and improvement of computing capacity (e.g., emergence of cloud computing platforms). While annual continental to global products of some land use/cover types have been created in a near-operational manner (e.g., forest, water, and urban) (Hansen et al., 2013; Pekel et al., 2016; Gong et al., 2020), frequent fine-scale irrigation mapping remains challenging due to the cryptic nature of the irrigation signal and the lack of ground reference data needed to train and validate machine learning and other classifiers. The data gaps are particularly problematic in the Midwestern and eastern US, where more abundant water resources have led to less concern and monitoring of irrigated land use.

This paper presents the newly created annual 30 m resolution irrigation maps and their comparisons with existing products. The maps (named LANID – Landsat-based Irrigation Dataset) cover the CONUS for the period of 1997–2017 and build upon a past effort of mapping for the year 2012 (Xie et al., 2019b), with key improvements in training sample generation, classification design, and accuracy assessment (Xie and Lark, 2021b). The maps presented here also include a newly mapped component – irrigated pasture and hay – that was not explicitly included in the preliminary version presented in Xie and Lark (2021b). In addition to the LANID maps, we present the collected ground truth data, which are particularly important for irrigation mapping efforts that require such a dataset to train or validate machine learning algorithms, especially where it has not been available in the humid eastern US. Additional products include maps of irrigation frequency, maximum extent, irrigation trends, and formerly and intermittently irrigated areas. In the following sections, we briefly review the methods used to generate these data and then present our maps and their comparisons with existing products that cover the entire US.

2 Methods

Our new LANID product contains 21 annual maps that characterize irrigation status of croplands, pasture, and hay across the CONUS for the years from 1997 to 2017. We first created annual maps of irrigated croplands (i.e., LANID_V1) using a supervised decision tree classification based on a novel training sample generation method and satellite-derived and environmental variables (see details in Xie and Lark, 2021b). Because LANID_V1 does not explicitly include irrigated pasture and hay, which is an important component of total irrigation, particularly in the western US, we addressed this limitation by applying the same machine learning method but using different mask layers and areal reference for training sample generation and classification (Fig. 1). The maximum extent of pasture and hay for the west was derived from the USGS National Land Cover Database (NLCD) and USDA Cropland Data Layer (CDL), identifying pixels that had been classified as pasture–hay in NLCD or non-alfalfa hay in CDL within any year between 1992 and 2017. To reduce competition between this pasture and hay mask and the one used for irrigated cropland mapping, we removed those pixels that had been classified as irrigated cropland in LANID_V1. The county-level areal reference of irrigated pasture and hay was calculated as the deficit of LANID_V1-based irrigated crop-

Table 1. Currently available irrigation maps covering part to the entire CONUS. The boldfaced maps are compared with LANID in the Results section (RF: random forest; RS: remote sensing).

Products	Spatial coverage	Resolution	Update frequency	Methods/datasets	Citations
Global Irrigated Area Map (GIAM)	Global	10 km rescaled to 1 km	Single map, 2000	Spectral matching/RS data	Thenkabail et al. (2009)
Global Map of Irrigation Areas (GMIA)	Global	10 km	5-year interval, 1995, 2000, and 2005	Spatial allocation/sub-nation statistics and maps	Siebert et al. (2005, 2013)
Synthesized map of global irrigated area	Global	1 km	Single map, covering 1999–2012	Decision tree/RS, GMIA, and land cover maps	Meier et al. (2018)
Global Food-Support Analysis Data (GFSAD)	Global	1 km	Single map, 2010	Spectral matching/RS time series	Teluguntla et al. (2015)
Global Land Cover Map (GlobCover)	Global	300 m	Single map, 2009	Automatic classification/ RS time series	ESA (2015)
Global Land Cover Characteristics (GLCC)	Global	1 km	Single map, 1992	Hybrid compositing techniques/RS data	Loveland et al. (2000)
Global Rainfed, Irrigated and Paddy Croplands (GRIPC)	Global	500 m	Single map, 2005	Decision tree/RS, climate, and ag. inventory data	Salmon et al. (2015)
MODIS-based Irrigated Agriculture Dataset (MIrAD)	CONUS	250 m	5-year interval, 2002–2017	Thresholding/agricultural census and RS data	Pervez and Brown (2010)
MODIS-based Irrigation Fraction (MIF)	CONUS	500 m	Single map, 2001	Decision tree/RS time series	Ozdogan and Gutman (2008)
USDA-NASS irrigation statistics	US	County-level	5-year interval, 1997–2017	Surveys	https://www.nass.usda.gov/AgCensus/index.php (last access: 15 April 2021)
USGS-verified irrigated lands	Western US	Field	Vary across states, 2002–2017	Visual interpretation/ RS and cropland inventory data	Brandt et al. (2021)
Landsat-based Irrigation Dataset 2012 (LANID 2012)	CONUS	30 m	Single map, circa 2012	RF/RS, climate, and environmental data	Xie et al. (2019b)
Annual Irrigation Maps – High Plains aquifer (AIM-HPA)	High Plains aquifer	30 m	Annual, 1984–2017	RF/RS, climate, and environmental data	Deines et al. (2019)
IrrMapper	Western CONUS	30 m	Annual, 1986–2018	RF/RS, climate, and environmental data	Ketchum et al. (2020)

land area compared to USDA-NASS-reported area, which includes all types of irrigated agriculture.

A key element of the LANID methodology is a novel way to generate training samples covering the entire country. To account for climate difference and mapping complexity, the CONUS was divided into western and eastern states based on a climatic transition near the 100th meridian, and training data were created corresponding to each region (Fig. 2). We used an automated method to generate training samples for the western states. For the years when USDA-NASS county-level irrigation statistics are available (i.e., 1997, 2002, 2007, 2012, and 2017), we adopted the thresholding method proposed by Xie et al. (2019b) to automate training sample generation, which assumed that irrigated lands appear greener

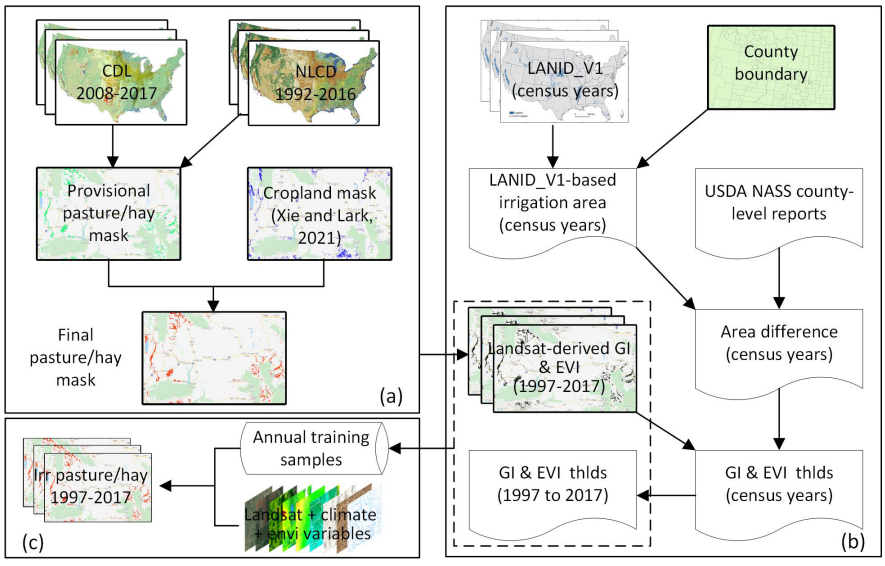

Figure 1. Flowchart of mapping irrigated pasture and hay in western US **(a)** generating the maximum extent of pasture–hay, **(b)** creating training samples, and **(c)** classification. Cropland mask refers to the maximum extent of non-pasture–hay cultivated land created in Xie and Lark (2021b).

than those that are rainfed. For non-census years, optimal thresholds were estimated based on relationships of crop greenness between non-census and census years. The calibrated and estimated thresholds were used to segment yearly maximum Landsat-based greenness index (GI) and enhanced vegetation index (EVI) to derive two intermediate irrigation maps per year, which were overlaid to identify consistent classification as potential training samples. As a result, the generated potential training samples were evenly distributed across the western CONUS on a yearly basis.

For the relatively humid eastern states, we visually collected samples through interpretation of multi-temporal very high-resolution images, street views, and time-series Landsat data on Google Earth and Google Earth Engine, based on the appearance of irrigation infrastructure such as wells, pipes, center pivot towers, and circular field patterns. Detailed methods of sample generation are described in Xie and Lark (2021b).

The predictors generally consist of two categories – satellite data and environmental variables (Xie and Lark, 2021b). The primary satellite-derived variables were calculated from all available Landsat images within each year, including yearly maximum, median, and range composites of GI, EVI, and normalized difference water index (NDWI). Annual and late-season (1 May to 15 October) sum of MODIS-derived indices (i.e., EVI and land surface temperature) were also used as additional variables. Environmental variables included annual and late-season sum of irrigation-relevant climate variables (i.e., precipitation, temperature, partial pressure of water vapor), elevation and slope, soil water content, and distance to major rivers (Deines et al., 2017, 2019; Xu et al., 2019; Xie et al., 2019b). Altogether, there were 32 input features (25 for the years 1997–2000 when MODIS products were not available).

Classification was implemented on Google Earth Engine, a cloud-computing platform that enables rapid accessing and processing of vast numbers of satellite images, climate data, and geophysical products (Gorelick et al., 2017). The classification was conducted annually per county using the widely used random forest classifier (Breiman, 2001). The county-level classifications were mosaicked to create an initial nationwide time-series irrigation map, followed by logic and spatial filtering to remove possible false classification (see details in Xie and Lark, 2021b).

3 Map evaluation and comparison design

Comprehensive assessment of nationwide irrigation maps is not possible without adequate ground truth data, especially for the eastern US. Therefore, accuracy of many published irrigation maps covering CONUS have been poorly evaluated. We compared our LANID maps to existing nationwide irrigation-specific maps, including two binary maps (i.e., MIrAD and GIAM) and two maps of irrigation fraction (i.e., MIF and GMIA areal percentage equipped for irrigation) (Table 1). Other global maps that include irrigation-related classes, such as Global Land Cover Map and GFSAD, are not shown because they are not irrigation-specific and substantially under-represent irrigation extent across the CONUS. In addition to coarser-resolution nationwide maps, we also compared our maps with recently available 30 m resolution maps for the High Plains aquifers and the 11 western states, i.e., AIM-HPA and IrrMapper, respectively.

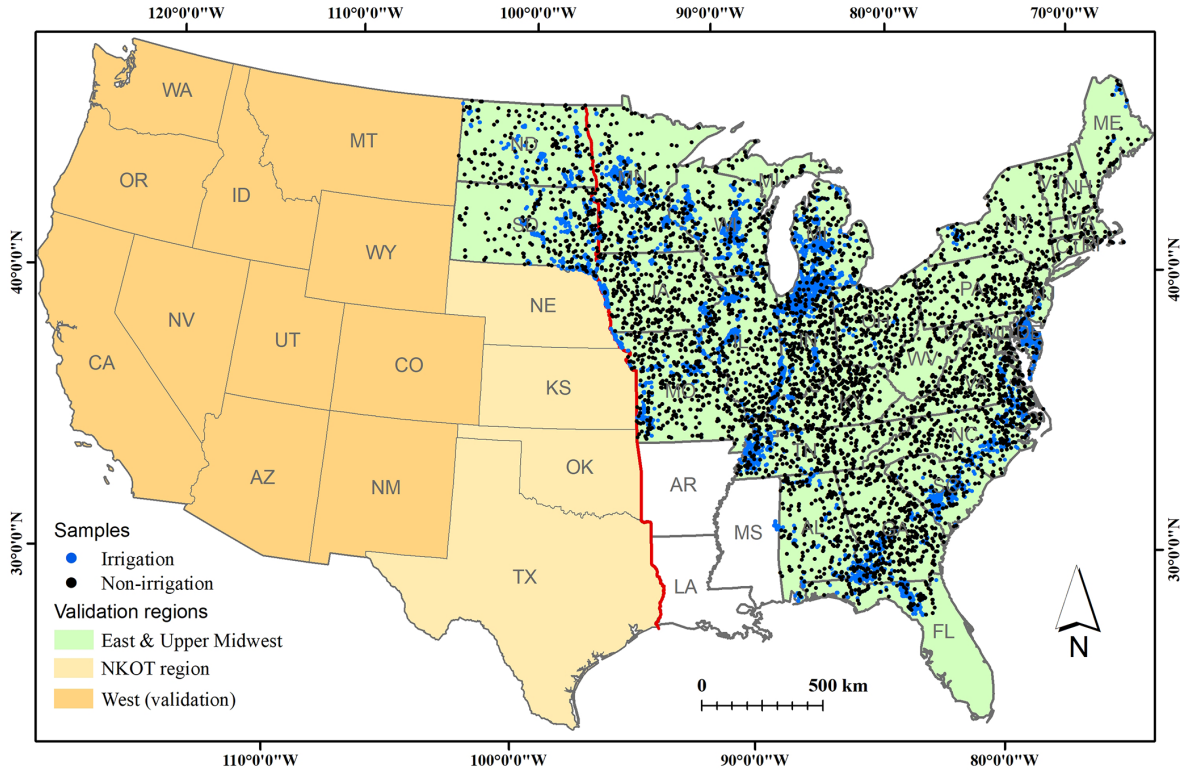

Figure 2. Map evaluation and comparison design and the distribution of test sample locations across the eastern CONUS. The NKOT region refers to Nebraska, Kansas, Oklahoma, and Texas, which covers the majority of the High Plains aquifer. The red solid line represents the west–east division for classification only.

Map evaluation and comparison were conducted by using test samples from two sources that cover the majority area of the CONUS – a published reference dataset from Ketchum et al. (2020) and an additional independent dataset that we collected for this study. The test samples from Ketchum et al. (2020) were collected through visual interpretation of field parcels based on irrigation clues from very high resolution images and crop greenness. The dataset has approximately 100 000 sample points, covering 11 western states (Fig. 2) for the whole study period of 1997–2017. Our independently collected validation samples (approximately 10 000 locations) covered the remaining areas except for Arkansas, Louisiana, and Mississippi. Lastly, we evaluated LANID's capability to detect irrigation change from pixel to state scales.

4 Results

4.1 Irrigation samples across the eastern US

To validate our maps, we collected approximately 10 000 irrigation and rainfed samples for the east (~ 5000 for each category) (Fig. 2). Each irrigation sample records a center pivot location and the presence of irrigation infrastructure during 1997–2017 (Fig. 3). In addition, we measured the radius of each center pivot irrigation system, i.e., the distance from its center to its field boundary. Note that the length of corner arms (designed for corner irrigation) was not measured (e.g., Field 1 in Fig. 3). Stable non-irrigation samples record the locations with clear evidence of no irrigation infrastructure during the entire mapping period. The average pivot radius for all samples collected in the eastern CONUS was 330 m, but distributed bimodally around approximately 200 and 400 m, which correspond respectively to broader rectangular circumscribed crop fields of 40 and 160 acres (16.19 and 64.75 ha), respectively.

4.2 Irrigation trends and changes

Our LANID reveals a steady increase in irrigated area throughout the CONUS, although there are some years with exceptional lower values – for example, 2012 and 2002, years in which there was significant drought (Fig. 4) (Otkin et al., 2018). Overall, irrigation area has increased by around 1.5×10^6 ha (Mha) during the period, from ~ 23 Mha before 2000 to ~ 24.5 Mha in 2016 with an average annual increase of ~ 80 000 ha. Consistent with earlier findings, the Central Valley of California, the High Plains portion of Texas, south-central Florida, and select western states (e.g., Utah, Colorado, Idaho, and Wyoming) experienced substantial irri-

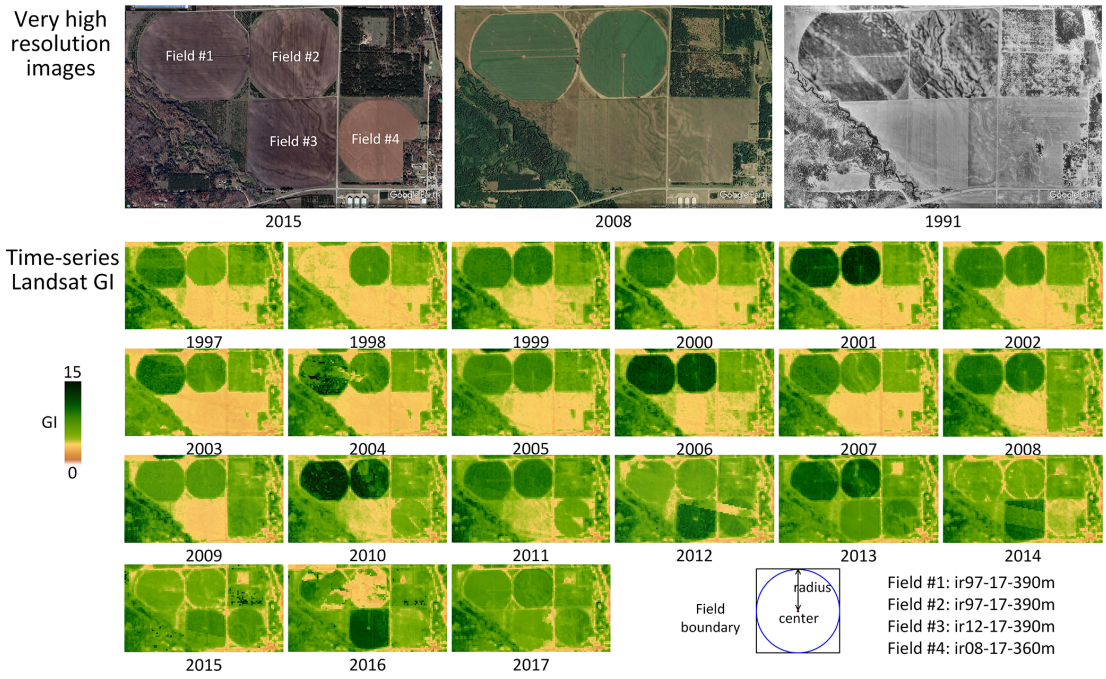

Figure 3. Demonstration of center-pivot irrigation field collection using very high-resolution time series (© Google Earth Pro 2021) and Landsat images. GI: greenness index.

gation loss during the period (per-state plots in Fig. 4). In contrast, irrigation increased in states across the Midwest (including Nebraska, North Dakota, and South Dakota), the Mississippi Alluvial Plain, and the East Coast. The largest gains occurred in Nebraska, Missouri, Michigan, Illinois, Arkansas, Mississippi, and Indiana, where irrigated area grew by over 100 000 ha per state.

Our LANID-derived irrigation changes agree well with USDA-NASS census-reported values (with R^2 from 0.81 to 0.96), indicating that LANID and the USDA-NASS data are consistent in their detection of irrigation change at both county and state scales. Relative to the NASS data, however, our LANID maps predict slightly greater irrigated extent at the national level and slightly fewer net changes at both state and county levels, especially for the eastern CONUS (Fig. 5).

Aggregating the annual LANID maps to a finer but still intermediate 6 km resolution can reveal more localized trends than state- or county-level data allow, while also accommodating for the field-level stochasticity and variations that often occur within a single farm or shared water source (Fig. 6). Such a resolution is particularly helpful for identifying small pockets of change with countervailing trends that would otherwise be masked or undetected. For example, we found outlier locations of irrigation loss in the Mississippi Alluvial Plain and of irrigation gain in the central and southern High Plains aquifer.

Ultimately, when applied at the highest resolution, our LANID maps can be used to reliably characterize irrigation dynamics at the sub-field- to field-level with overall accuracy and kappa index of 81 % and 0.62, respectively (Table 2). For instance, sub-field to field level expansions, losses, and interannual variations in irrigation that are detectable from LANID can be clearly observed in north Texas (Fig. 7a). Although such a level of change detection in more humid areas is not as effective as more arid states due to a weaker contrast between irrigated and rainfed fields, LANID still provides a reasonable and accurate characterization of irrigation change through time there as well, as shown in the example in Michigan (Fig. 7b).

Table 2. Accuracy of change detection using LANID maps. Change is defined as frequency difference between the two sub-periods (i.e., 1998–2007 and 2008–2017) greater than 3, and the stable class refers to the value smaller than or equal to 3. Note non-agriculture is excluded from the stable class.

		Reference		
		Stable	Change	User's accuracy
Classified	Stable	187	63	75 %
	change	13	137	91 %
	Producer's accuracy	94 %	69 %	
Overall accuracy: 81 %; kappa: 0.62				

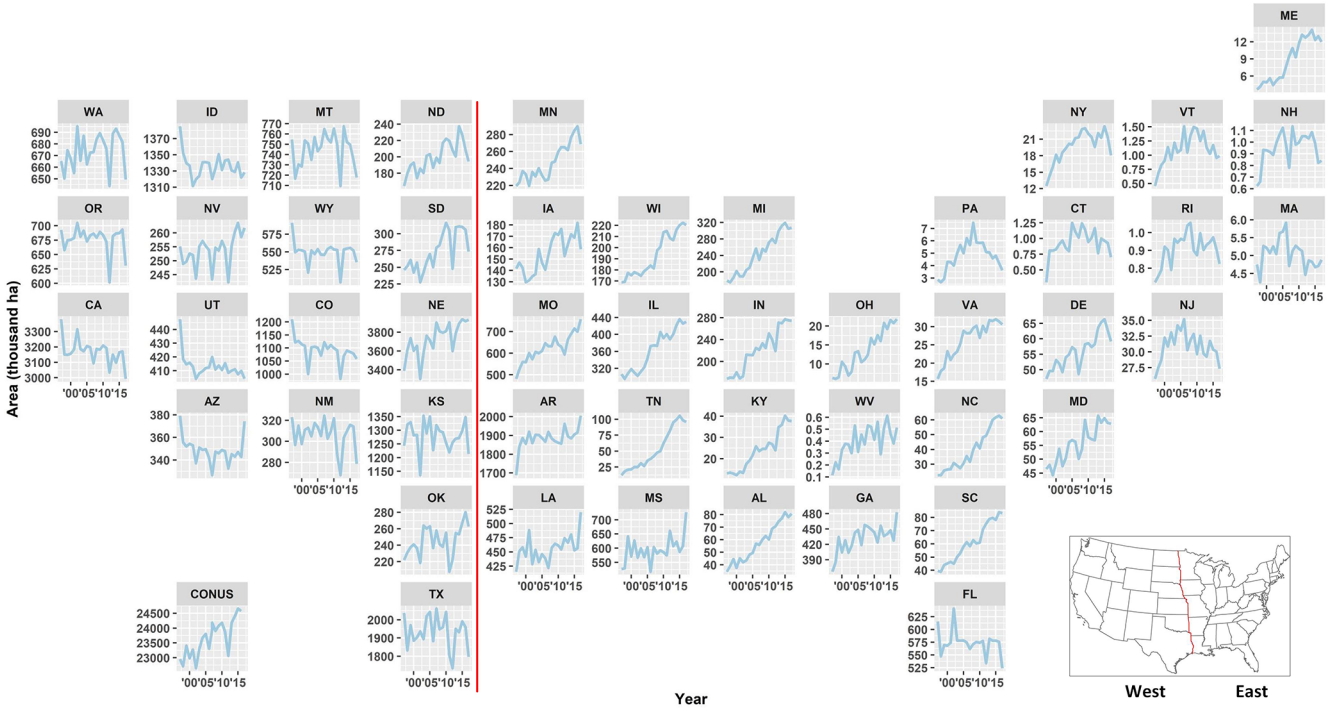

Figure 4. LANID-derived annual irrigation area by state, 1997–2017. The red line shows the east–west division in this study based on a climatic transition near the 100th meridian. Annual irrigation area per state is provided in Table A1.

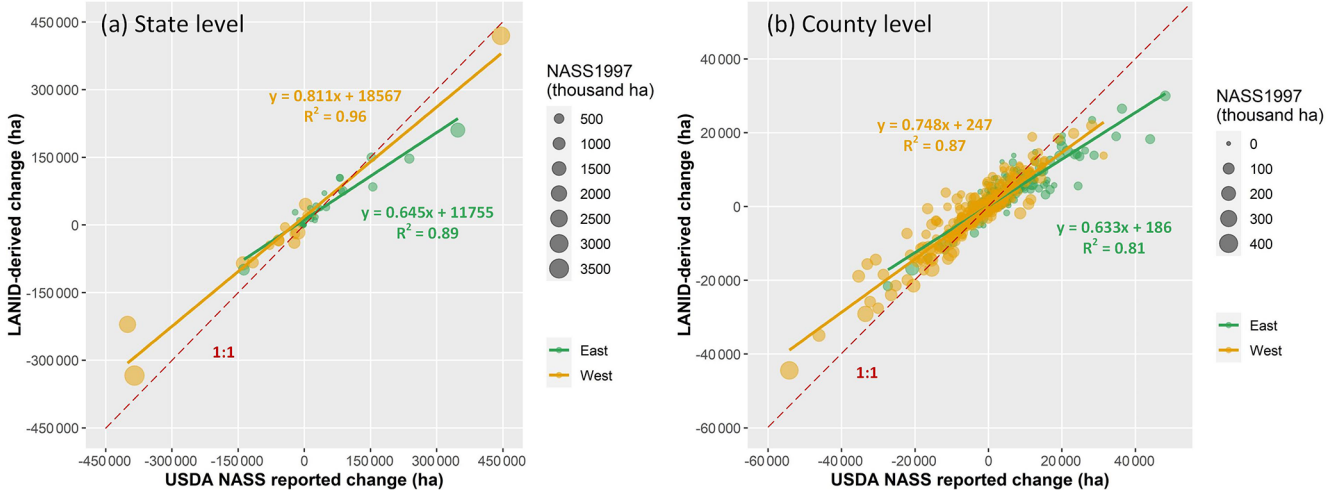

Figure 5. LANID-derived irrigation changes vs. USDA-NASS-reported area at the state **(a)** and county **(b)** scales. Irrigation change was calculated as the difference between mean area of the years 2012 and 2017 and that of 1997 and 2002 (i.e., mean($\text{irArea}_{2012} + \text{irArea}_{2017}$) − mean($\text{irArea}_{1997} + \text{irArea}_{2002}$), where irArea_{yr} refers to irrigation area of year). The USDA-NASS-reported values of 1997 are shown to represent irrigation area at the starting point of the study period.

4.3 Irrigated pasture and hay

This study provides the first complete mapping and delineation of irrigated pasture and hay for the western US (Fig. 8). In this region, forage and fodder crops provide valuable feed for livestock, and irrigation is often necessary to cultivate certain species or attain viable yields. This contrasts with pasture and hay in the eastern states, where annual precipitation and soil moisture are typically sufficient for robust production of grass-based forage and fodder. Areas of irrigated pasture and hay have a pattern of land use distinct from that of irrigated croplands, as well as unique implications for water use and the environment.

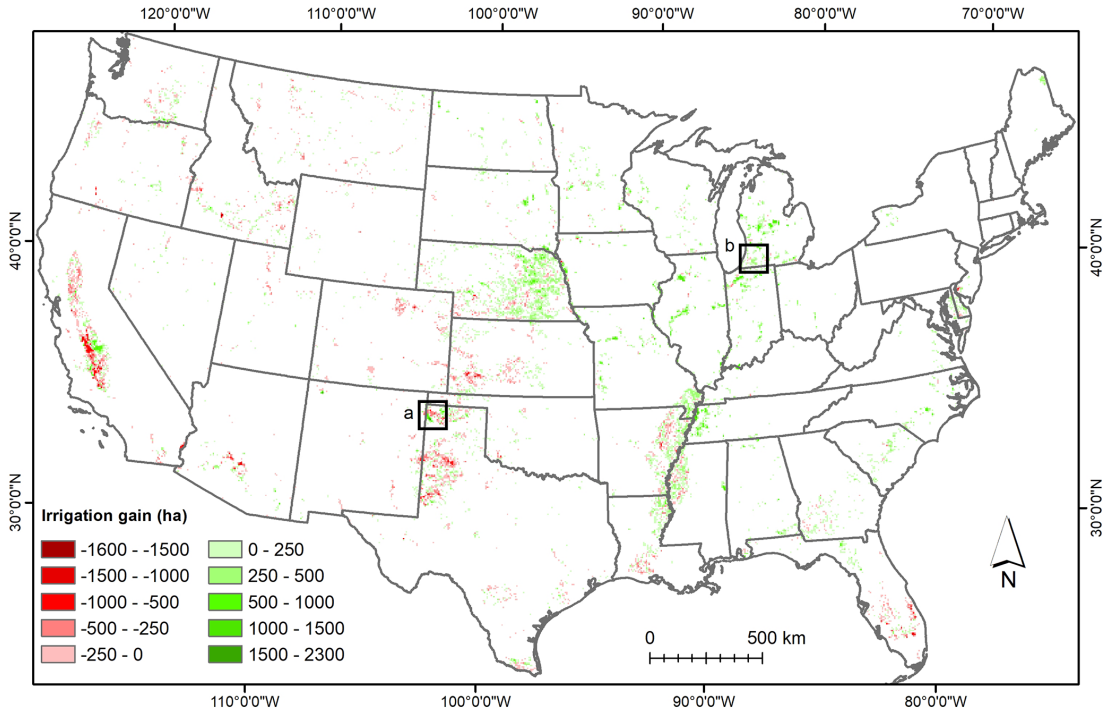

Figure 6. LANID-derived irrigation gain from 1998–2007 to 2008–2017 at the 6 km × 6 km scale. Per-grid value is calculated as the difference between mean irrigation area of 1998–2007 and that of 2008–2017 (i.e., $\text{meanIrArea}_{2008-2017} - \text{meanIrArea}_{1998-2007}$, where irArea is LANID-aggregated irrigation area within a 6 km × 6 km grid). Grids with absolute change < 2.5 % are shown as background.

Compared to the first version of LANID, which did not explicitly include irrigated pasture–hay, we found an average of 0.34 Mha more irrigated land (i.e., more irrigated pasture and hay included in LANID_V2 compared to LANID_V1) for the years 2013 to 2017 and a similarly larger amount (0.36 Mha) since the start of the study period. This increase in irrigated extent is lower than that of the USDA census of Agriculture's estimate of 1 Mha of irrigated pasture – the only other spatial (but coarse) estimate of such irrigated land use (Sanderson et al., 2012). The difference between our annual estimates and that of the census data likely reflects the fact that a large portion of irrigated pasture and hay (especially alfalfa) had already been mapped in the first version of LANID. To confirm this, we further calculated a direct estimate of only irrigated pasture–hay as all irrigated pixels classified as pasture or hay in the NLCD or CDL and estimated an average area of 1.39 Mha across the years 2008, 2011, 2013, and 2016. This estimate is 0.39 Mha higher than the 1 Mha reported by the Census of Agricultural but includes both pasture and hay, whereas the census estimate is for pasture only.

4.4 Maximum extent, frequency, and formerly and intermittently irrigated land

Across all types of irrigation – including cultivated cropland and pasture and hay – a total of 38.5 Mha of land was irrigated at least one time between 1997 and 2017, representing the maximum irrigated extent in the US for our study period (Fig. 9a and Table 3). Of these areas, just 24.2 Mha (62.8 %) was irrigated in 2017, and this annual utilization percentage ranged from 58.8 % to 64.0 % over the full study period. Across all pixels within the maximum irrigated extent, the mean annual irrigated frequency was 12.9 out of 21 years (Fig. 9b). The distribution of irrigated frequency suggests many areas consist of stable, persistent irrigation but that there also exists a substantial amount of land with intermittent irrigation use. Those pixels with the very lowest irrigation frequency likely reflect locations where irrigation ceased very early in the study period or was first initiated very late in the study period, and/or areas of potential misclassification.

Looking at the subset of lands that are no longer irrigated, we found 4 Mha of formerly irrigated land (i.e., not irrigated anytime in the most recent 3 years, 2015–2017, but that was irrigated at least three times prior) (Table 3). This formerly irrigated land is primarily distributed across the western states (as shown in Fig. 6) and may reflect areas where insufficient water availability has limited the ongoing use, or where salination of soils, socioeconomic drivers, or other superseding factors have resulted in a cessation of irrigated agriculture. Of these formerly irrigated areas, 71.6 % remains in crop production under rainfed conditions, primarily planted for corn (13.2 %), soybeans (12.3 %), and spring–winter wheat

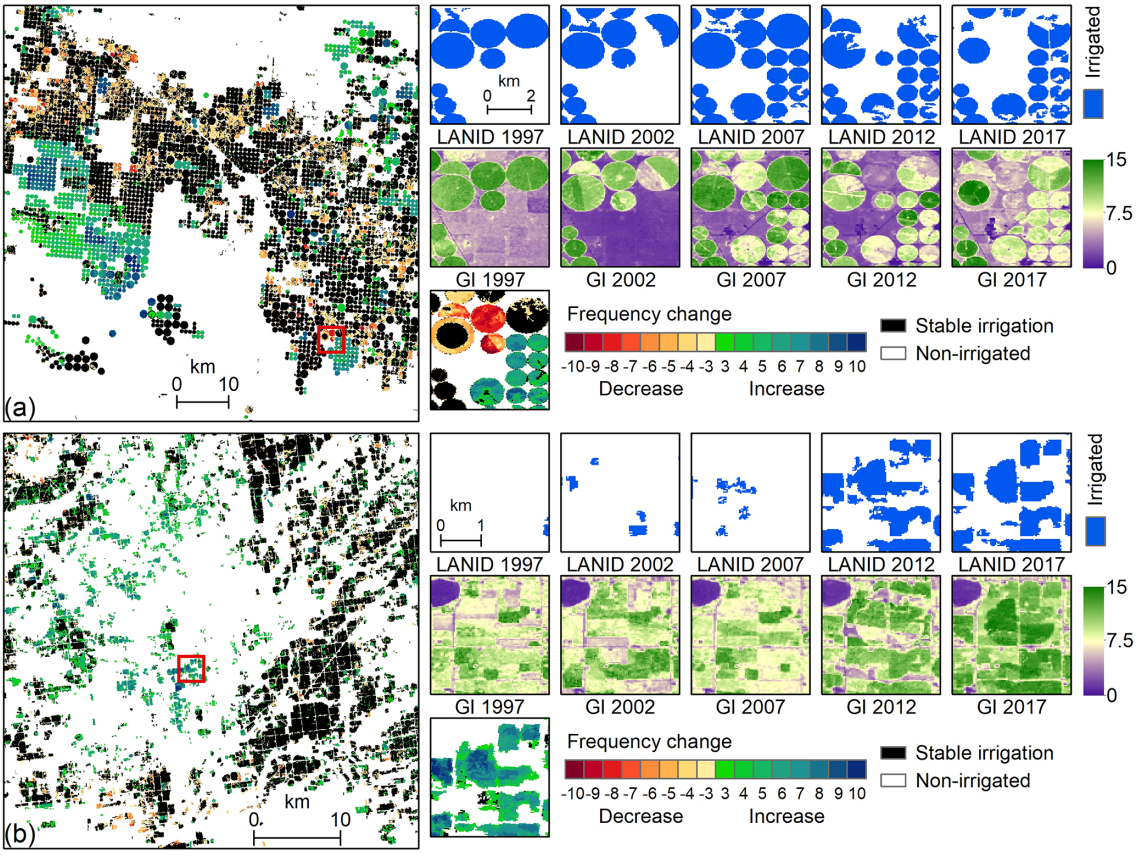

Figure 7. Demonstration of LANID-derived field-level irrigation frequency change for the northern Texas **(a)** and southwestern Michigan **(b)** (highlighted in Fig. 6). Frequency change refers to the difference of number of years irrigated between 1998–2007 and that between 2008–2017 (i.e., $\text{irFreq}_{2008-2017} - \text{irFreq}_{1998-2007}$, where irFreq is the number of years irrigated).

Table 3. Statistics of irrigation area (in 10^6 ha) across the CONUS for the period 1997–2017.

		Area	Definition
Average annual area		23.7	Mean annual irrigation area
Maximum area		38.5	Irrigated at least once
Formerly irrigated		4.0	Not irrigated anytime in 2015–2017, but irrigated at least three times prior
Long-term irrigation	Intermittently irrigated	13.5	Irrigated at least once for both 1997–1999 and 2015–2017, and irrigation frequency ≤ 18
	Continuously irrigated	12.0	Irrigated at least once for both 1997–1999 and 2015–2017, and irrigation frequency > 18

(12.2 %) as of 2017. The remaining locations have either been abandoned from cultivated crop production altogether (26.3 %) or converted to urban use (2.1 %). Those areas for which an irrigated crop is no longer viable may represent an opportunity for farmers to transition to grassland-based agriculture (Deines et al., 2020), for example via the introduction of pasture for livestock grazing or the harvesting of biomass for use as forage or cellulosic bioenergy feedstock (Robertson et al., 2017). As climate change and decreasing freshwater availability continue to strain water resources, the total area of formerly irrigated lands is likely to increase, thereby creating even further opportunity and greater need for alternative drought-resistant agricultural opportunities, such as those afforded by perennial feedstock production.

In addition to those locations where irrigation has ceased completely, we observed a substantial amount of land where

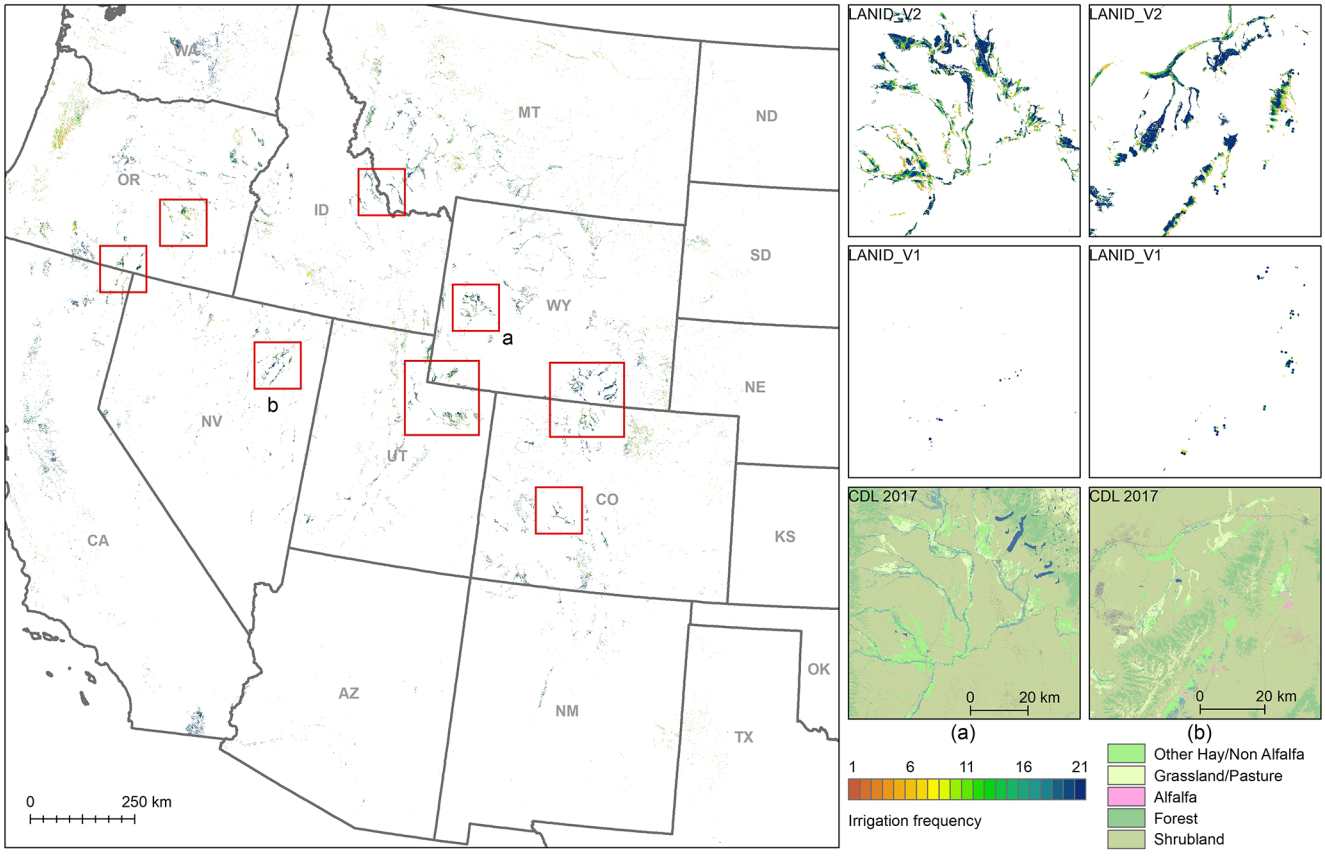

Figure 8. Distribution of irrigated pasture and hay derived from LANID_V2 (presented in this study) in the western CONUS. The overview shows irrigation frequency (i.e., the number of years a pixel is irrigated during 1997–2017). The highlighted areas in the red rectangles represent areas of intensively irrigated pasture and hay that were not completely mapped in LANID_V1. Panels **(a)** and **(b)** are examples of local views for western Wyoming and northeastern Nevada, respectively.

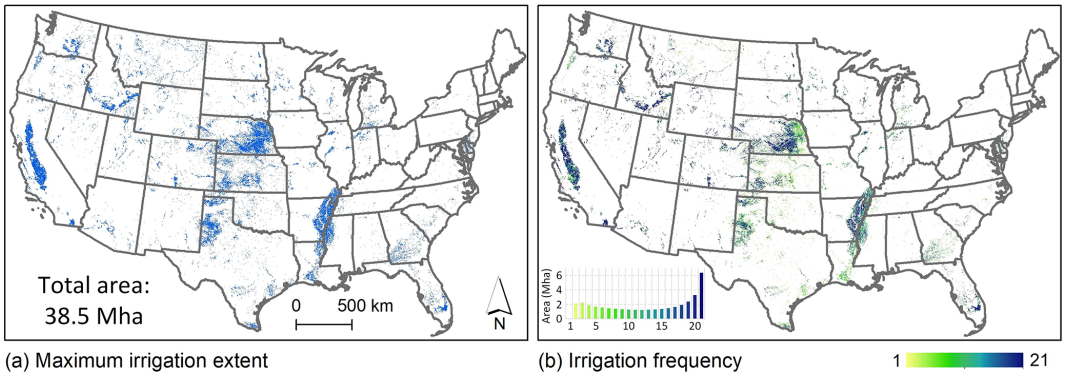

Figure 9. The maximum irrigation extent (lands that have been irrigated at least once) and irrigation frequency (the number of irrigated years) across the CONUS for the period 1997–2017. The inset in **(b)** shows the area of each frequency value.

irrigation remained active in the most recent years but where its use across time was discontinuous. For example, we found 25.5 Mha of land across the CONUS that had been irrigated spanning the whole study period (i.e., irrigated at least once for both 1997–1999 and 2015–2017), where over half of that subset (i.e., 13.5 Mha) could be best described as intermittently irrigated (frequency $\leq$ 18) (Table 3). As opposed to those locations with continuous annual irrigation use or where irrigation has ceased altogether, these intermittently irrigated lands appear to remain in irrigated agriculture today yet rely on such irrigation use just 67 % (median value) of the time across the 21-year study period. While further in-

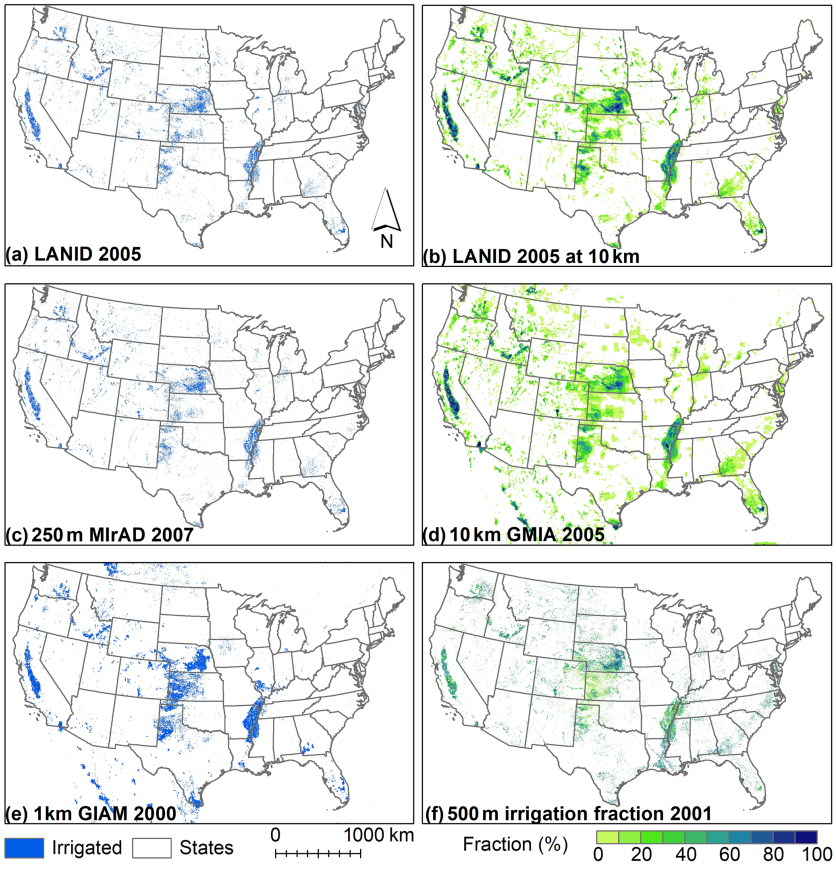

Figure 10. Nationwide views of different irrigation mapping products. LANID 2005 is aggregated to 1 **(a)** and 10 km **(d)** resolution for comparison purposes. The LANID-derived irrigation frequency refers to the number of years a pixel is classified as "irrigated".

vestigation is needed to better characterize these areas of partial irrigation use over time, it may be possible that they represent locations where irrigation is only supplemental (e.g., used only in dry years or when needed), shared among a single water source but rotated among multiple nearby fields, or used only in years with sufficient water availability or water application rights and allocations. Similar to formerly irrigated lands, these locations of intermittent irrigation application may present areas of opportunity or economic need for alternative rainfed agriculture in non-irrigated years. In such cases, drought-tolerant annual crops like forage or energy sorghum could potentially provide economic opportunities for producers and limited further strain on local hydrology (Enciso et al., 2015; Mullet et al., 2014; Cui et al., 2018).

4.5 Comparisons with existing products

Figure 10 presents the nationwide view of a single year LANID as well as other irrigation-specific products. The 30 m LANID 2005 map was aggregated to 10 km resolution (Fig. 10b) for comparing with other coarser-resolution maps. Across broad scales, all maps show similar irrigation hotspots of the High Plains aquifer, the Central Valley aquifer, the Mississippi Alluvial Plain, the Snake River aquifer, and the East Coast. While it might be reasonable to conclude that all these coarse-resolution maps can capture similar irrigation patterns at the national scale, regional views emphasize the details that are uniquely captured by LANID. For instance, LANID identifies fewer irrigated pixels at the eastern Columbia Plateau aquifer than other maps, especially compared to MIF and GIAM (Fig. 11). In another example of the High Plains aquifer, GIAM and MIF substantially overestimate irrigation extent in western and central Kansas compared to both LANID and MIrAD (Fig. 12). Among all comparison products, MIrAD provides the most similarity of irrigation patterns as LANID in the arid to semi-arid west and Midwest.

In more humid areas like the upper Midwest, our LANID map captures patterns that are considerably misclassified by other maps (Fig. 13). For example, GIAM and MIF omit the majority of irrigated fields in the region; MIrAD shows a clear administrative boundary effect and near-random distribution of irrigation within each county. At 10 km resolution, GMIA provides similar patterns as LANID but exaggerates the overall irrigation extent.

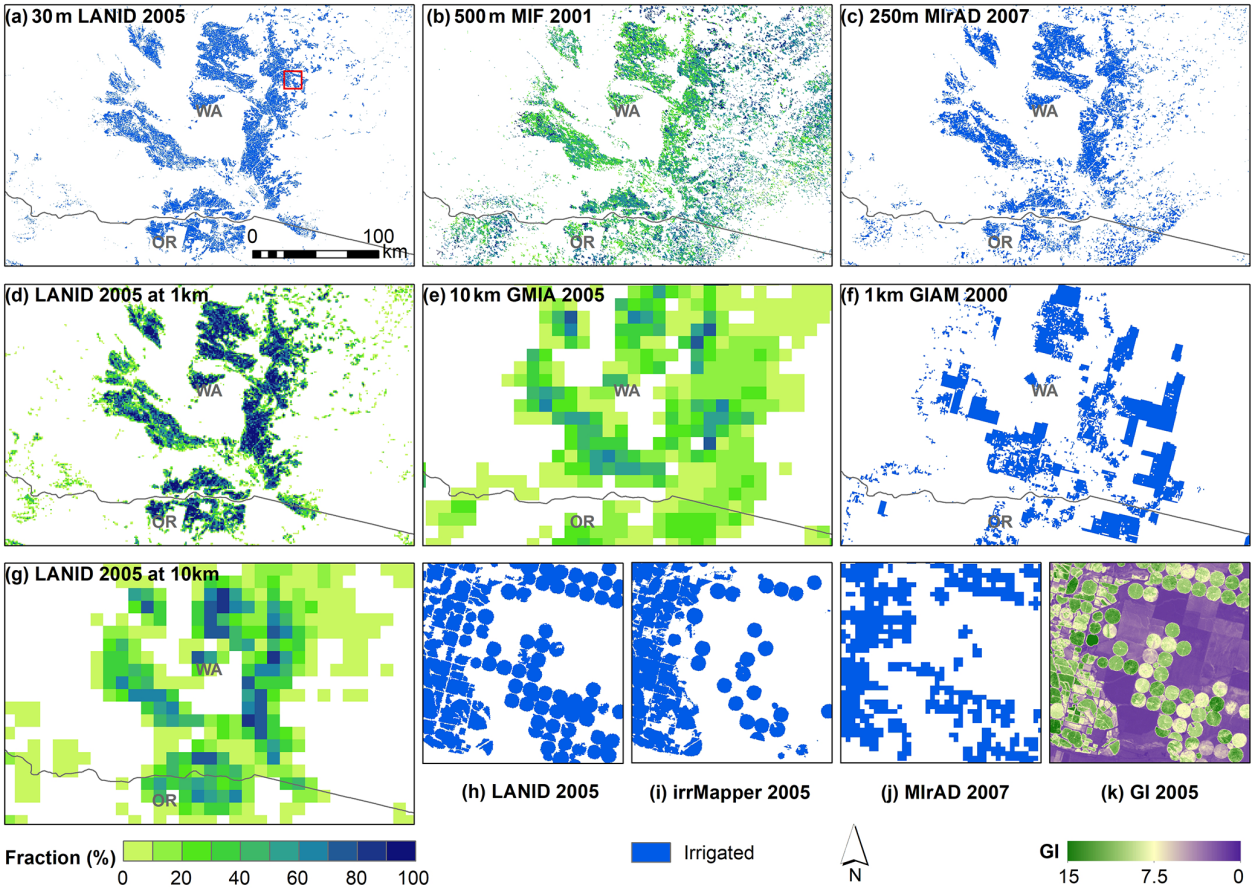

Figure 11. Product comparison at the Columbia Plateau Aquifer in northern Oregon and southern Washington. In addition to the original 30 m LANID **(a)**, the map is aggregated to 1 and 10 km resolution for panels **(d)** and **(g)**. Panels **(h–i)** show the location highlighted in **(a)** (red rectangle).

Locally, LANID shows a substantial improvement of spatial detail compared to other maps. For example, boundaries of center pivot and rectangular fields are clearly recognizable in LANID, while they are obscured even on the 250 m resolution MIrAD (insets (h) and (j) of Figs. 11 and 12). It is also evident that LANID shows comparable spatial details as other regional maps IrrMapper and AIM-HPA (inset (i) of Figs. 11 and 12) while still offering consistent and comprehensive coverage across the CONUS.

At the state level, our LANID estimates are consistent with USDA-NASS-reported data (Fig. 14b), although the agreement is weaker than that of products like MIrAD and GMIA, which both rely directly and exclusively on census data as areal reference (not shown in the figure). In contrast, MIF underestimates irrigated area at the state level (Fig. 14c), whereas GIAM substantially overestimates irrigation extent, especially for the states with reported area greater than 10^6 ha (Fig. 14d).

The results of pixel-based assessment further reveal the advantages of LANID over other nationwide maps (Table 4). We find that the overall accuracy is generally high for the NKOT region (i.e., Nebraska, Kansas, Oklahoma, and Texas) across all nationwide maps except for GIAM, with mean accuracy ranging from 78.9 % (MIF) to over 95 % (the LANID maps). Similarly, all maps show relatively high overall accuracy for the 11 western states, with values ranging from 82.6 % of MIF to 94.2 % of MIrAD. Despite these maps' reasonable accuracy in the west and even Midwest, they incorrectly assign a considerable number of rainfed fields as irrigated possibly due to coarse resolution and their difficulty separating them in some areas such as the Columbia Plateau aquifer (Fig. 11). For example, GIAM captures many low-density pixels in the west (Fig. 15c); MIF overestimates the locations with irrigation fraction between 0 % and 60 % (Fig. 15b); MIrAD maps irrigated pixels with a median fraction around 80 % (Fig. 15a).

In the eastern US, our LANID maps stand out with overall accuracy of 94.4 % – on par with their performance in the western US – whereas other maps show accuracy below 60 %. The extremely low accuracy of MIrAD, MIF, and GIAM in the east is attributable to their missing of most irrigated cropland as well as frequent false identification

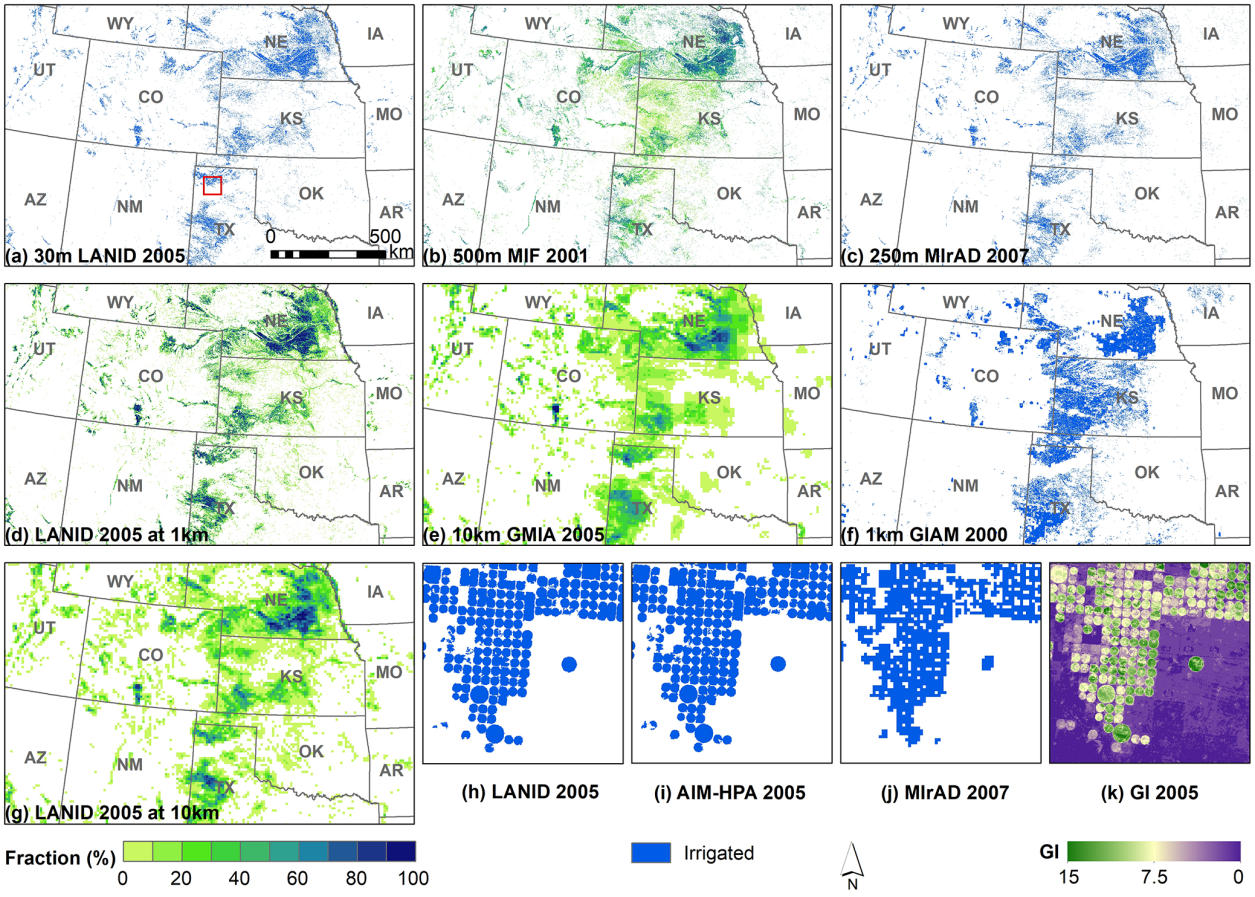

Figure 12. Product comparison at the High Plains aquifer. In addition to the original 30 m LANID **(a)**, the map is aggregated to 1 and 10 km resolution for panels **(d)** and **(g)**. Panels **(h–i)** show the location highlighted in **(a)** (red rectangle).

of rainfed cropland as irrigated (see Fig. 13 as an example), as characterized by omission error rates of over 80 % and commission error rates of over 45 % for the "irrigated" and "non-irrigated" classes, respectively. As a result, MIrAD maps irrigated pixels in the east that have a median irrigated fraction of about 50 % according to LANID (Fig. 15a); GIAM misclassifies a substantial number of low-density pixels (Fig. 15c); MIF substantially overestimates the locations with an irrigation fraction beyond 30 % (Fig. 15b).

We also compared our maps to AIM-HPA (i.e., Annual Irrigation Maps – High Plains aquifer) (Deines et al., 2019), a dataset with the same spatial and temporal resolution as LANID but covering only the High Plains aquifer. In this region, LANID performs comparably to the HPA-specific dataset, with overall accuracy of 95.9 % vs. 93.2 %, respectively, and kappa values of 0.89 vs. 0.82.

For a broader region with the 11 western states, our LANID maps show 92.8 % congruence (kappa of 0.84) with the reference data from IrrMapper (Ketchum et al., 2020) compared to a 99.1 % (kappa of 0.98) congruence of the IrrMapper product with its reference data. Such results follow in part from the methods of reference data utilization, as IrrMapper used 60 % of the validation data used in our comparison for its classifier training. Further differences between LANID and IrrMapper may stem from differences in sampled data and irrigated class definition. For example, the IrrMapper point-based irrigation samples were stratified from verified fields that were digitized in years different from the time of irrigation verification, such that they likely capture permanently irrigated croplands well but may potentially include fields that are partially irrigated or fallowed in any given year. In addition, IrrMapper's reference irrigation samples appear to include both irrigated croplands and other grass-like lands, such as irrigated turfgrass and groundwater- or fluvially subsidized grasslands and wetlands. This broader and more variable pool of reference data may thus help explain additional observed differences, such as occasionally less distinct field boundaries in IrrMapper compared with LANID and GI (e.g., left-hand portions of Fig. 11h–k) as well as the slightly higher apparent accuracy of MIrAD (which relies only on vegetation greenness) compared to LANID in the west when assessed against the IrrMapper reference data (Table 4). Thus, while overall performances of LANID and other datasets are similar in overlapping re-

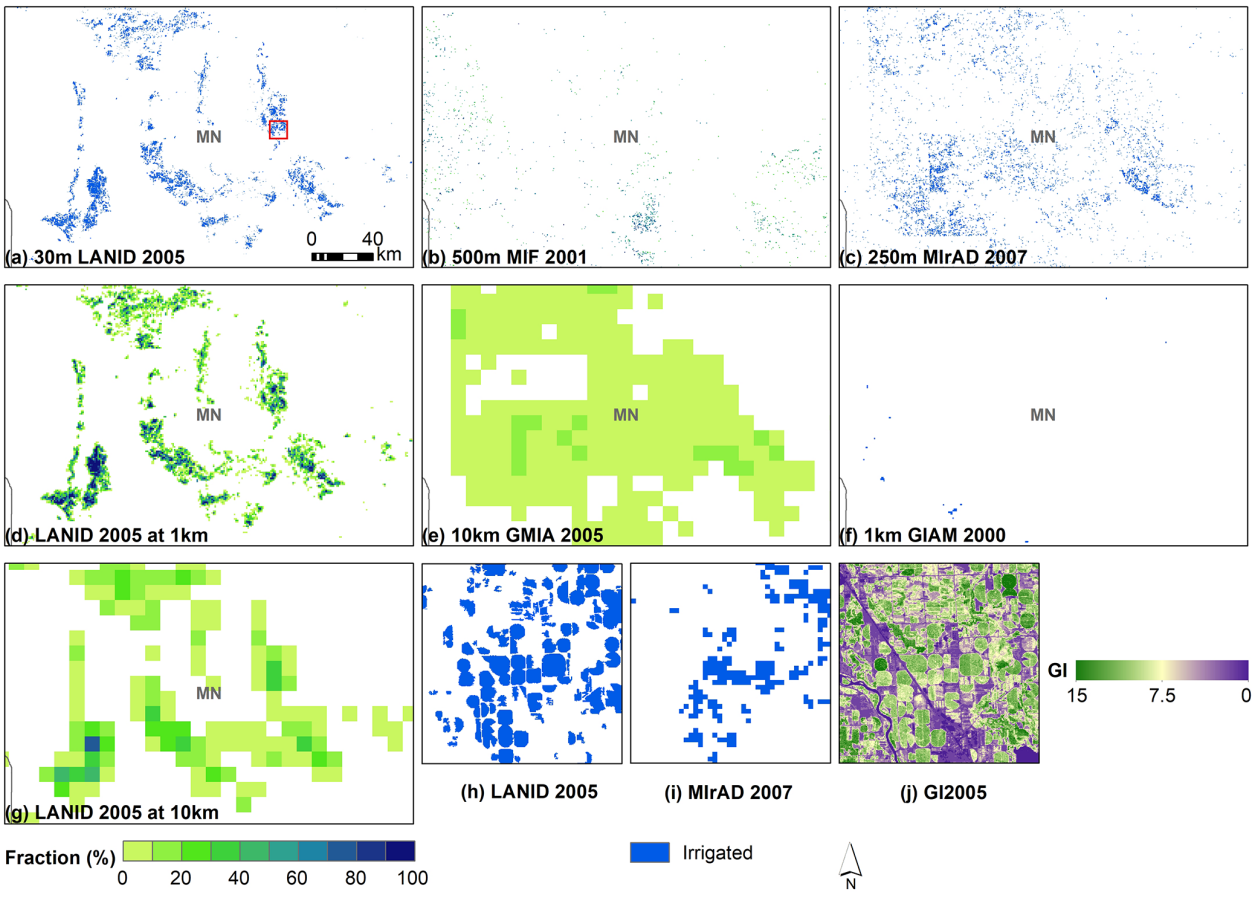

Figure 13. Product comparison in central Minnesota. In addition to the original 30 m LANID **(a)**, the map is aggregated to 1 and 10 km resolution for panels **(d)** and **(g)**. Panels **(h–i)** show the location highlighted in **(a)** (red rectangle).

gions like the HPA and the western states, differences in each product's intent and class specificity will likely dictate preferences for specific user applications.

5 Discussion

5.1 Uncertainty, limitations, and future improvements

Both qualitative and quantitative assessments show extensive improvements of LANID compared to other currently available nationwide maps in terms of spatial detail and temporal frequency. Despite the advances, caution is still needed, especially when applying the dataset at the scale of individual fields in the eastern US. For example, mapping accuracy in the Mississippi Alluvial Plain region is uncertain due to the absence of reference data and the difficulty of collecting aerial ground truth in the area. In addition, map accuracy in the humid east is slightly lower than in the arid and semi-arid west. The quality of maps might also vary over time due to availability of clear Landsat observations. For instance, fewer Landsat images in 2012 constrained map quality, and scan-off effects of the ETM+ sensor might remain in some areas.

We took several post-classification steps to improve mapping accuracy, which also introduces limitations to LANID. First, our minimum mapping unit of 5 acres (2.02 ha) (i.e., 23 Landsat pixels) improved mapping confidence but also excluded smaller irrigated fields, such as fragmented irrigated vegetable fields often found in suburban and peri-urban areas. Second, the assumption that fields equipped with irrigation systems tend to be cropped and irrigated frequently could have incorrectly masked out some irrigated fields historically under long-term and frequent fallow conditions (e.g., irrigated – long-term fallow conditions – irrigated). Lastly, our current version of LANID covers only the period of 1997 to 2017, which might be problematic for users who want maps outside the study period. However, we hope to regularly update the existing dataset in the future to include the most recent years of available imagery, and, if able, extend the time series back in time through the duration of the Landsat record.

Given these uncertainties and limitations, future generations of LANID could benefit from the following improvements. First, we anticipate using our temporally extendable methodology to routinely update LANID, such that cover-

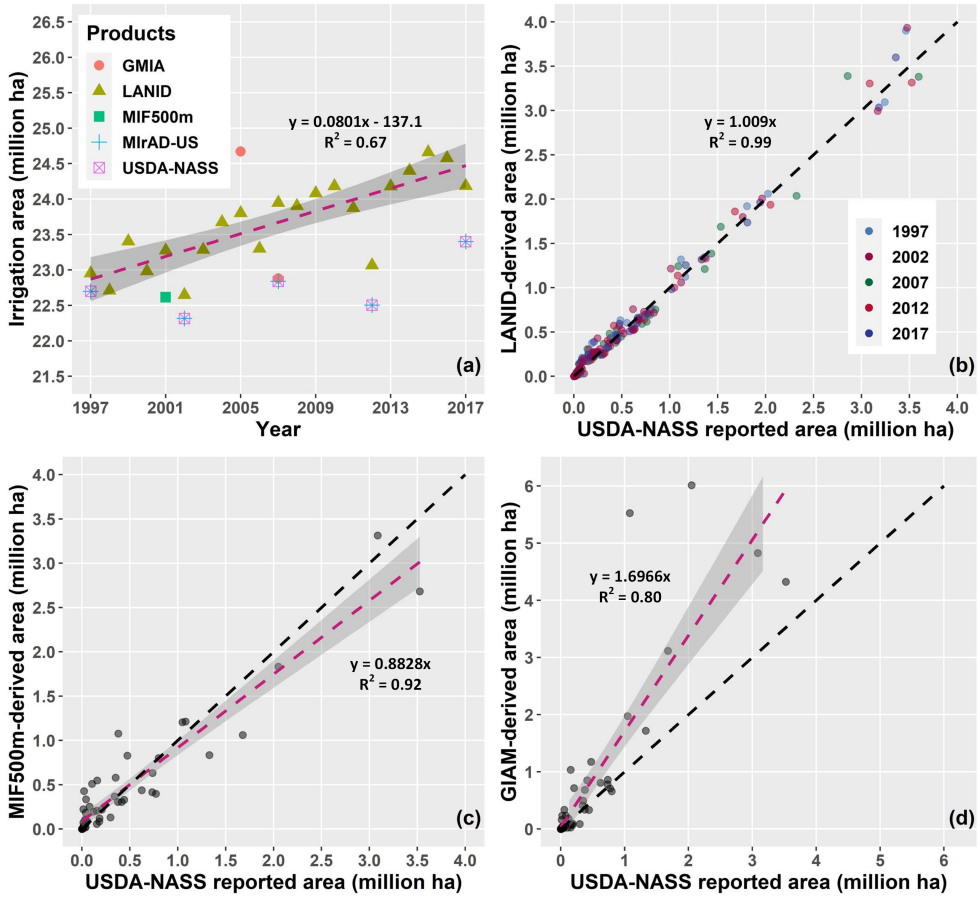

Figure 14. Comparisons of irrigated area between products at the nation **(a)** and state **(b–d)** levels. **(a)** LANID-derived nationwide irrigation trend (dashed pink line) and irrigated area of other products. **(b)** USDA-NASS-reported vs. LANID-estimated irrigation area for 5 census years. **(c)** USDA-NASS-reported (2002) vs. MODIS-estimated (2001) irrigated area (adapted from Ozdogan and Gutman, 2008). **(d)** USDA-NASS reported (2002) vs. GIAM-estimated (2000) irrigated area. Note the GIAM-estimated nationwide irrigated area (39×10^6 ha) is not shown in **(a)** due to its exceptionally high value. State-level comparisons between USDA-NASS and MIrAD-US and GMIA are not demonstrated because both products used census data as reference.

age could extend prior to 1997 and up to the most recent year. Efforts could also be made to enhance spatial detail (e.g., 10 m resolution) and mapping accuracy, particularly in the humid eastern US where contrasts between irrigated and rainfed crops are obscure. This is practical for recent years when both the revisit frequency and spatial resolution of satellite observations are greatly improved. Lastly, implementation of an irrigation-specific change detection algorithm could help improve the identification and consistency of monitoring variations in irrigation over time.

5.2 Potential applications

Our annual 30 m resolution nationwide LANID maps may be valuable to local, state, and regional water governance bodies, agribusinesses, and the research community for a variety of applications including water use estimation, risk assessment, use as model input, and more.

Our LANID maps could benefit water and agricultural managers by providing insights into irrigation changes (e.g., expansion and abandonment) at geographic and temporal scales relevant to decision-making. Our field-scale, wall-to-wall data will enable local and regional water management organizations, which may not otherwise have sufficient data or resources, to make better decisions that influence regional water availability. For example, state-level water managers and engineers who need to plan how much water to allocate for agriculture could utilize our irrigation distribution and change information to estimate demand. Policy makers may also use LANID to navigate future decision making and to evaluate federal agricultural, bioenergy, and conservation policies (Mccarthy et al., 2020; Lark, 2020).

Our dataset may also be useful for agribusinesses and entities across agricultural supply chains. For example, our maps could be used by companies that seek to reduce risk from water scarcity within their supply chains or lower the water foot-

Table 4. Confusion table of pixel-wise accuracy assessment. The overall accuracy, omission error (1 – producer's accuracy), and commission error (1 – user's accuracy) are in percent. Accuracy values are averaged if multiple-year assessment was conducted. Parenthetical numbers represent the standard deviation.

Maps	Region	Year	Kappa	Overall accuracy	Omission error		Commission error		Sample size	Irrigation sample
					Irrigated	Non-irr.	Irrigated	Non-irr.		
LANID	West[a]	1997–2017	0.84 (0.07)	92.8 (3.5)	11.4 (6.9)	3.6 (1.0)	6.1 (4.9)	10.7 (8.9)	4433	2284
	NKOT	1997–2017	0.93 (0.02)	96.6 (0.8)	5.9 (1.4)	1.0 (0.2)	1.0 (0.2)	5.6 (1.3)	9994	5002
	East	1997–2017	0.89 (0.01)	94.4 (0.6)	10.7 (1.2)	0.5 (0.1)	0.6 (0.1)	9.7 (1.0)	10 000	5000
	HPA[b]	1997–2017	0.89 (0.03)	95.9 (1.1)	4.7 (1.4)	2.3 (0.6)	0.7 (0.2)	13.0 (3.3)	5890	4479
MIrAD	West[a]	2002, 2007	0.84 (0.02)	94.2 (0.8)	10.3 (2.4)	4.3 (0.9)	11.2 (5.4)	4.3 (2.1)	3102	987
	NKOT	2002, 2007, 2012, 2017	0.76 (0.05)	87.8 (2.5)	18.0 (4.4)	6.3 (0.7)	7.1 (1.0)	16.2 (3.4)	9967	5014
	East	2002, 2007, 2012, 2017	0.16 (0.01)	58.0 (0.7)	82.3 (1.1)	1.7 (0.6)	8.7 (2.9)	45.6 (0.4)	10 000	5000
MIF[c]	West[a]	2001	0.49	82.6	47.8	7.4	29.9	14.6	3002	747
	NKOT	2001	0.58	78.9	27.2	14.9	17.0	24.3	9985	5001
	East	2001	0.12	55.9	83.6	4.6	21.9	46.7	10 000	5000
GIAM	West[a]	2000	0.72	87.6	23.5	6.2	12.6	12.3	3436	1234
	NKOT	2000	0.25	62.6	57.2	17.5	29.0	41.0	10 040	5023
	East[a]	2000	0.04	52.2	93.5	2.0	23.6	48.8	10 000	5000
AIM-HPA	HPA[b]	1997–2017	0.82 (0.04)	93.2 (1.8)	6.9 (2.4)	6.4 (3.4)	2.1 (1.1)	18.6 (4.8)	5890	4479
	HPA[d]	1997–2017	–	92.7 (1.5)	14.0 (4.5)	3.1 (1.7)	8.5 (2.1)	8.5 (2.1)	1316	519
IrrMapper	West[a]	1997–2017	0.98 (0.01)	99.1 (0.3)	0.3 (0.2)	1.4 (0.3)	2.4 (1.9)	0.3 (0.2)	4433	2284
LANID2012	NKOT	2012	0.84	92.0	10.1	5.8	6.0	9.8	9938	5002
	East	2012	0.49	74.4	49.4	1.9	3.7	33.5	10 000	5000

[a] Validation samples from Ketchum et al. (2020). Test samples for the years 1999, 2004, 2005, 2012, 2015, and 2017 were not used because of limited irrigated samples. [b] Validation samples from this study. [c] Irrigated pixels were set as a fraction greater than 20 %. [d] Accuracy assessment reported by Deines et al. (2019). NKOT: Nebraska, Kansas, Oklahoma, and Texas.

print of their sourced products (Brauman et al., 2020). Additional applications may include business decision-making and financial investment (Turral et al., 2010), precise field-level water use estimation and solutions (Sadler et al., 2005), and crop yield prediction and its water resilience (Troy et al., 2015).

A key informant and collaborator in the development of our LANID maps has been the USGS, and the produced outputs may help support several ongoing USGS efforts, such as the National Water Census's efforts to provide water budgets at the watershed level (USGS, 2020a), the National Water-Use Information Program (NWUIP) dissemination of water use data (USGS, 2020b), and the Water Availability and Use Science Program (WAUSP) assessments of regional groundwater availability (USGS, 2020c). The research community within USGS also has high-priority goals to improve quantification of crop consumptive water use and project future water use. Our improved estimates of irrigation location, extent, and dynamics could help refine evapotranspiration estimates of irrigated croplands, thereby improving estimates of agricultural water use from field to aquifer scales and further supporting the ongoing expansion of detailed water use estimates across the continental US (Senay et al., 2016, 2017).

We also hope that our dataset will serve several needs in the broader research community, especially for those who study hydrology, agriculture, and the environment from local to nationwide scales. For example, our 30 m resolution irrigation data could be used to potentially improve the classification accuracy of or add irrigation status to existing USGS and USDA land cover maps (Brown et al., 2020; Lark et al., 2021; Wickham et al., 2021), investigate the relationships among irrigation changes and cropland expansion and abandonment (Lark et al., 2020; Yin et al., 2020), or explore the competition and biophysical interactions between irrigated agriculture and urban expansion (Xie et al., 2019a; Van Vliet, 2019; Bren D'amour et al., 2017). Users of previous coarser-resolution irrigation datasets will also benefit from the improvements in spatial detail, product frequency, and map accuracy. Existing nationwide irrigation datasets like MIrAD have been accessed by hundreds of users in academia and government via the USGS EROS website (Brown and Pervez, 2014). These data have been incorporated into studies to evaluate trends in ground and surface water quality,

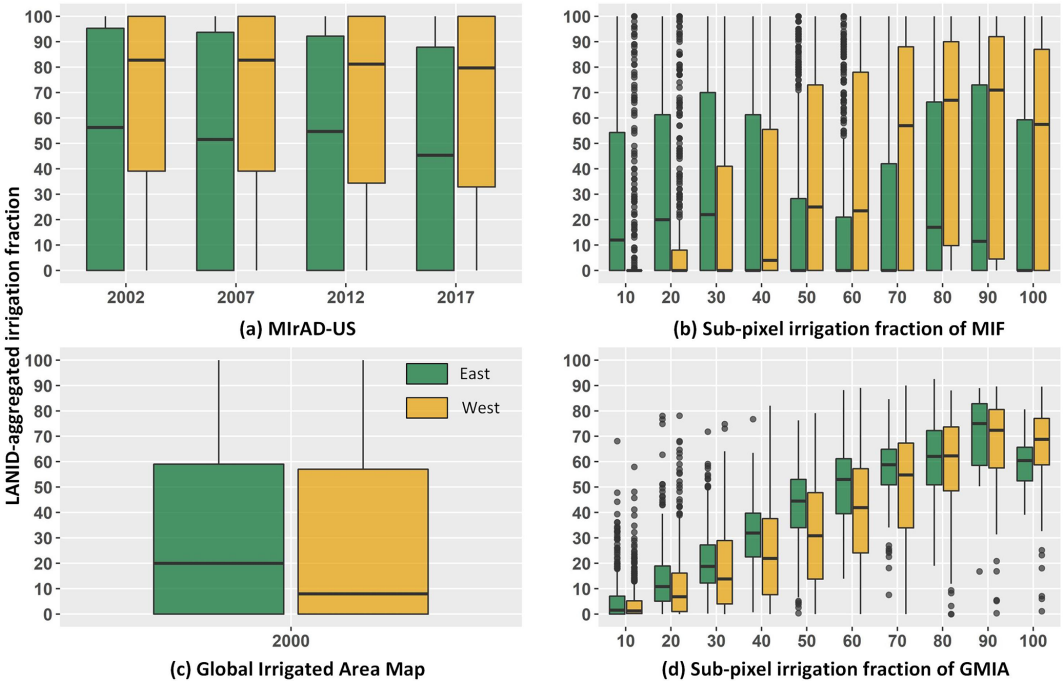

Figure 15. Box plots showing irrigation fraction mapped in each product using LANID as reference. The western and eastern CONUS (separated by red line in Fig. 2) are shown as brown and green, respectively. The 30 m LANID maps were aggregated as an irrigation fraction to match the spatial resolution of each product (e.g., 250 m for MIrAD). For binary maps MIrAD and GIAM, 5000 irrigated samples were stratified for both west and east; 50 samples were selected for each irrigation fraction from 1 % to 100 % (with increments of 1 %) in MIF and GMIA. The numbers on the horizontal axes of **(b)** and **(d)** refer to the maximum value of each bin.

model evapotranspiration, and energy–water exchange at the surface boundary layer, and they reveal locations at risk of unsustainable irrigation (Brown and Pervez, 2014; Pryor et al., 2016; Seyoum and Milewski, 2016; Jin et al., 2011; Zaussinger et al., 2019). Our 30 m data products will enhance similar types of applications and enable many others through the improved spatial and temporal resolution. To this extent, several organizations have begun using our previously published LANID 2012 for further research and development activities, despite there being only 1 of the presently described 21 annual years of data available; such applications should be further enabled by the current full suite of products and time periods.

Lastly, our collected samples could help generate new threads of irrigation maps for the eastern US. Because insufficient ground reference data have long been a bottleneck to producing accurate classifiers for irrigation mapping, our verified locations could facilitate the development and evaluation of new models for irrigation detection, especially when other constraints are becoming relieved due to increasingly available high- to moderate-resolution remote sensing images, development of machine learning algorithms, and open access of cloud computing platforms.

6 Data availability

Our annual LANID maps, their byproducts (i.e., maximum irrigation extent, irrigation frequency, and per-pixel irrigation trends), ∼ 10 000 manually collected ground reference data, and metadata can be accessed via https://doi.org/10.5281/zenodo.5548555 (Xie and Lark, 2021a). All maps use the Albers equal-area conical projection at 30 m resolution except for the map of irrigation trends of 6 km.

7 Conclusions

This paper presents the only annual, nationwide fine-resolution maps of irrigation extent for the US, which are available for each year from 1997–2017, and offer several improvements over other products. The increased resolution of the described LANID dataset sets a new standard in spatial detail at the CONUS extent, while the increased mapping frequency and multidecadal coverage enable characterization of irrigation dynamics. Our accuracy assessment shows that the LANID maps provide the most realistic depiction of irrigation extent across the country, with performance that matches or exceeds existing regional datasets.

Moving forward, the LANID maps provide a foundation for refined representations of irrigation distribution and dy-

namics across the US. It is clear from recent research efforts that high-quality, frequently updated data on fine-scale irrigation extent are immensely valuable for both the research and application user communities. With these needs in mind, our future intents and interests surrounding LANID may focus on (1) routinely updating annual maps after 2017, (2) providing finer-resolution maps of irrigation extent (e.g., 10 m) by fusing multi-source imagery, and (3) improving mapping accuracy in the eastern CONUS.

Appendix A

Table A1. The LANID-derived state-level irrigated area (in hectares) of each year between 1997 and 2017.

1997–2008											
States	1997	1998	1999	2000	2001	2002	2003	2004	2005	2006	2007
Alabama	34 535	39 125	44 618	37 601	45 173	42 095	43 512	48 210	49 533	56 837	55 946
Arizona	379 287	355 684	352 011	354 327	353 060	337 113	351 052	348 990	349 530	342 038	326 403
Arkansas	1 687 799	1 839 858	1 886 084	1 855 790	1 920 171	1 859 224	1 903 682	1 902 655	1 886 089	1 866 404	1 919 269
California	3 380 488	3 151 686	3 149 145	3 156 261	3 184 521	3 314 552	3 187 264	3 172 349	3 206 905	3 197 729	3 094 285
Colorado	1 210 321	1 121 823	1 127 185	1 114 290	1 108 564	1 000 578	1 102 934	1 105 161	1 100 720	1 070 917	1 121 951
Connecticut	302	807	807	829	910	970	851	801	1251	1108	1013
Delaware	47 054	49 638	49 591	53 128	52 042	49 221	53 965	54 924	57 305	56 429	48 586
Florida	615 570	547 328	569 116	568 295	574 083	640 918	578 654	578 092	578 447	574 716	561 719
Georgia	366 690	384 742	434 499	404 428	428 114	403 744	416 991	442 892	448 528	418 726	457 852
Idaho	1 385 130	1 352 224	1 339 614	1 336 683	1 311 422	1 319 562	1 323 663	1 340 630	1 340 766	1 339 902	1 319 951
Illinois	306 516	295 264	308 291	318 324	309 793	302 484	312 484	322 255	343 074	372 371	374 335
Indiana	168 572	170 884	170 226	180 406	169 450	173 272	212 469	211 910	211 605	224 793	221 168
Iowa	141 592	146 916	142 392	129 494	131 310	134 782	136 684	158 873	146 813	140 562	153 320
Kansas	1 243 244	1 321 112	1 329 850	1 282 021	1 283 028	1 135 702	1 353 488	1 288 916	1 350 727	1 227 553	1 318 920
Kentucky	13 104	13 479	12 991	12 209	13 955	13 346	17 538	19 164	21 688	25 816	23 551
Louisiana	415 211	451 161	458 231	442 128	488 285	428 395	453 754	432 163	445 974	438 908	421 933
Maine	3644	4142	4983	4910	5629	4403	5167	5738	5731	7701	9487
Maryland	46 450	47 965	44 192	48 584	53 744	47 490	50 384	56 148	56 940	56 354	50 152
Massachusetts	4756	4250	5274	5216	5069	5258	5044	5629	5670	5920	4709
Michigan	179 126	174 745	186 417	202 131	189 431	189 615	204 443	210 328	233 991	256 992	229 009
Minnesota	219 513	223 631	236 929	233 381	219 645	236 085	230 768	240 468	232 043	225 834	227 401
Mississippi	526 481	529 629	641 770	570 773	627 065	567 028	599 802	568 687	603 644	517 243	604 432
Missouri	480 854	523 644	559 171	558 573	600 994	571 590	605 685	600 251	610 383	646 444	632 748
Montana	754 784	716 614	730 501	728 447	753 781	750 609	734 975	756 981	743 386	747 750	764 726
Nebraska	3 388 881	3 607 761	3 737 425	3 602 001	3 655 262	3 303 885	3 577 851	3 763 770	3 713 858	3 628 089	3 902 377
Nevada	255 173	248 903	249 718	252 576	252 090	243 633	255 082	257 084	255 298	253 798	243 299
New Hampshire	625	661	934	930	918	891	991	1065	1123	976	782
New Jersey	25 712	27 451	28 717	32 253	30 855	33 095	31 175	34 197	33 369	35 184	30 257
New Mexico	323 098	296 609	314 995	297 562	310 916	312 938	304 907	317 588	313 720	305 273	324 526
New York	12 503	14 324	15 970	18 173	16 761	18 620	19 341	20 163	20 029	21 209	21 336
North Carolina	22 569	22 641	25 847	26 482	26 672	30 930	29 181	27 337	30 732	35 506	31 644
North Dakota	164 616	179 741	190 039	192 953	174 264	185 754	180 438	201 479	203 502	186 949	199 093
Ohio	6345	6091	6492	10 584	9362	6949	7985	12 980	13 365	10 487	11 161
Oklahoma	221 859	230 949	237 608	240 967	236 309	218 499	263 921	260 352	263 092	236 626	257 870
Oregon	693 065	657 674	674 871	675 721	678 911	705 284	681 086	691 636	672 903	683 382	686 578
Pennsylvania	2877	2648	2918	4303	4295	4006	4970	5664	5006	6213	5665
Rhode Island	721	755	790	921	903	791	965	944	965	958	1039
South Carolina	39 571	38 942	44 011	45 249	46 390	45 040	50 078	53 012	57 992	61 285	58 224
South Dakota	245 846	251 604	260 802	241 994	256 887	227 293	242 316	257 936	269 721	250 017	279 162
Tennessee	12 096	18 410	20 843	21 540	24 923	25 049	30 954	26 660	34 988	37 998	42 068
Texas	2 037 060	1 832 083	1 970 036	1 886 396	1 902 613	1 935 970	1 894 429	2 020 246	2 042 627	1 883 622	2 061 213
Utah	447 520	418 494	414 730	415 852	412 975	404 106	408 105	409 668	411 897	412 424	420 019
Vermont	459	675	827	905	1143	918	1219	1048	1090	1508	1047
Virginia	15 675	17 807	18 575	23 268	20 898	22 374	23 122	25 289	28 893	28 187	28 249
Washington	665 353	650 243	674 586	666 842	654 969	695 216	665 695	687 093	662 436	672 477	672 925
West Virginia	115	224	165	328	378	373	300	531	312	455	373
Wisconsin	168 788	169 200	177 363	175 174	177 969	176 654	174 700	179 013	181 334	183 905	181 335
Wyoming	591 280	549 623	552 916	552 251	550 526	520 762	552 083	546 981	553 945	546 109	545 747
CONUS	22 952 830	22 709 864	23 405 066	22 983 454	23 276 428	22 647 066	23 286 147	23 673 951	23 802 940	23 301 684	23 948 855

Table A1. Continued.

2009–2017										
States	2008	2009	2010	2011	2012	2013	2014	2015	2016	2017
Alabama	60 139	63 088	60 198	68 873	70 572	74 533	76 987	81 990	78 022	80 805
Arizona	347 354	345 935	348 800	347 701	332 402	345 229	342 976	347 084	342 758	374 399
Arkansas	1 884 322	1 869 713	1 862 017	1 856 051	1 962 000	1 895 565	1 884 232	1 904 854	1 915 934	2 005 406
California	3 188 969	3 183 257	3 210 136	3 193 344	3 034 074	3 150 194	3 098 087	3 165 015	3 171 492	2 993 121
Colorado	1 097 294	1 111 432	1 099 495	1 090 921	982 058	1 069 911	1 090 256	1 085 316	1 079 062	1 058 369
Connecticut	1240	1146	946	1011	1167	766	1000	964	930	704
Delaware	53 855	58 197	58 583	57 379	58 263	63 623	65 377	66 345	62 686	59 182
Florida	571 469	575 663	574 039	577 377	533 861	581 562	577 921	578 069	575 584	524 110
Georgia	454 795	449 800	443 450	423 956	456 294	436 233	440 079	447 356	427 585	482 965
Idaho	1 332 914	1 350 822	1 331 055	1 342 894	1 343 860	1 330 616	1 328 663	1 340 649	1 321 842	1 328 081
Illinois	373 296	405 632	391 193	401 018	388 723	400 631	422 017	435 894	425 569	429 765
Indiana	232 998	224 904	251 318	239 992	219 071	271 049	269 836	277 084	274 989	274 193
Iowa	165 879	172 773	171 304	176 592	152 614	162 926	171 756	168 785	181 923	158 593
Kansas	1 298 163	1 293 371	1 254 278	1 219 387	1 255 779	1 269 960	1 271 563	1 298 644	1 348 197	1 213 904
Kentucky	24 637	24 648	27 565	26 845	23 918	34 820	35 942	40 236	37 892	37 695
Louisiana	457 305	464 418	461 525	454 552	474 357	466 391	480 660	453 071	456 294	520 158
Maine	10 911	9281	11 768	13 246	12 731	13 232	14 101	12 322	12 993	12 004
Maryland	53 551	64 218	57 960	57 262	56 885	65 756	63 208	64 878	63 111	62 859
Massachusetts	5127	5277	5190	5125	4462	4867	4829	4676	4710	4883
Michigan	255 967	249 827	271 441	280 475	270 287	298 783	312 146	319 282	304 834	307 379
Minnesota	246 865	248 258	259 921	265 191	265 084	261 758	276 892	284 753	289 736	268 822
Mississippi	581 096	592 122	586 089	574 756	661 108	607 189	623 127	586 732	607 843	727 048
Missouri	632 621	677 098	639 719	630 628	594 163	663 467	689 456	714 821	700 031	757 763
Montana	755 680	751 866	765 259	749 722	709 597	767 409	752 198	749 607	734 882	717 839
Nebraska	3 809 427	3 795 113	3 812 085	3 906 419	3 599 322	3 788 075	3 890 195	3 938 095	3 916 648	3 932 941
Nevada	254 701	253 634	257 118	254 508	242 259	255 488	260 470	263 629	258 504	261 773
New Hampshire	1136	979	998	1051	1052	1033	1086	989	824	841
New Jersey	31 874	32 858	29 627	32 556	29 711	29 231	31 729	30 367	30 056	27 307
New Mexico	302 674	309 613	322 031	287 084	267 775	303 436	309 672	315 822	314 231	278 521
New York	22 813	22 985	21 997	21 375	19 613	22 087	21 278	23 348	21 348	18 062
North Carolina	39 903	44 633	40 770	48 174	49 348	54 476	60 055	61 742	62 867	60 946
North Dakota	192 548	216 921	222 074	219 590	208 126	200 636	237 311	227 049	208 587	194 485
Ohio	12 389	16 820	15 163	17 568	16 019	20 830	19 226	21 596	20 769	21 797
Oklahoma	241 465	237 963	255 306	207 626	222 411	254 679	253 346	267 197	280 375	262 775
Oregon	679 313	689 700	683 527	672 638	601 796	681 881	686 693	687 199	693 521	630 691
Pennsylvania	7463	5875	5829	5862	5100	5071	4593	4810	4193	3633
Rhode Island	1055	899	873	996	903	931	947	973	907	825
South Carolina	62 819	60 304	60 997	70 816	75 314	78 853	79 582	78 073	83 985	83 152
South Dakota	282 989	300 158	316 604	305 400	247 765	310 061	311 233	310 428	306 264	273 417
Tennessee	47 716	50 000	62 366	72 275	82 320	95 120	99 624	105 668	98 550	95 929
Texas	1 947 439	1 958 584	2 042 729	1 806 539	1 734 962	1 950 095	1 931 265	1 990 790	1 960 109	1 797 103
Utah	410 925	413 886	410 487	415 526	408 438	409 979	411 089	407 372	409 971	404 194
Vermont	1343	1497	1467	1250	1429	1135	1024	1176	953	988
Virginia	29 632	30 258	26 965	30 214	28 495	31 826	31 587	32 060	31 459	30 626
Washington	684 029	689 341	683 064	675 888	643 850	688 835	693 133	687 186	681 781	649 433
West Virginia	532	521	413	562	291	511	614	462	381	515
Wisconsin	197 534	200 655	213 834	214 935	208 410	206 657	216 340	220 279	222 335	220 264
Wyoming	554 241	556 873	553 396	552 743	506 874	553 539	554 765	555 745	552 047	535 443
CONUS	23 902 407	24 082 816	24 182 969	23 875 893	23 064 913	24 180 935	24 400 166	24 660 482	24 579 564	24 185 708

Author contributions. YX created the dataset, wrote the original draft, and reviewed and edited the manuscript. HKG reviewed and edited the manuscript. TJL acquired funding and reviewed and edited the manuscript. All authors have reviewed and agreed on the published version of the paper.

Competing interests. The contact author has declared that neither they nor their co-authors have any competing interests.

Disclaimer. Any use of trade, firm, or product names is for descriptive purposes only and does not imply endorsement by the US government.

Acknowledgements. The authors would like to thank members of the USGS Water Budget and Estimation Project for sharing verified irrigation data, feedback and ideas for mapping, and insights regarding data use for water estimation. We also appreciate the comments from the anonymous reviewers and editors and their helpful suggestions.

Financial support. This research has been supported by the US Geological Survey (grant no. G19AC00080) and the US Department of Energy (grant no. DE-SC0018409).

Review statement. This paper was edited by David Carlson and reviewed by two anonymous referees.

References

Brandt, J. T., Caldwell, R. R., Haynes, J. V., Painter, J. A., and Read, A. L.: Verified Irrigated Agricultural Lands for the United States, 2002–17, U.S. Geological Survey data release [data set], https://doi.org/10.5066/P9NAWU1U, 2021.

Brauman, K. A., Goodkind, A. L., Kim, T., Pelton, R. E. O., Schmitt, J., and Smith, T. M.: Unique water scarcity footprints and water risks in US meat and ethanol supply chains identified via subnational commodity flows, Environ. Res. Lett., 15, 105018, https://doi.org/10.1088/1748-9326/ab9a6a, 2020.

Breiman, L.: Random forests, Mach. Learn., 45, 5–32, 2001.

Bren d'Amour, C., Reitsma, F., Baiocchi, G., Barthel, S., Guneralp, B., Erb, K. H., Haberl, H., Creutzig, F., and Seto, K. C.: Future urban land expansion and implications for global croplands, P. Natl. Acad. Sci. USA, 114, 8939–8944, https://doi.org/10.1073/pnas.1606036114, 2017.

Brown, J. F. and Pervez, M. S.: Merging remote sensing data and national agricultural statistics to model change in irrigated agriculture, Agr. Syst., 127, 28–40, https://doi.org/10.1016/j.agsy.2014.01.004, 2014.

Brown, J. F., Tollerud, H. J., Barber, C. P., Zhou, Q., Dwyer, J. L., Vogelmann, J. E., Loveland, T. R., Woodcock, C. E., Stehman, S. V., Zhu, Z., Pengra, B. W., Smith, K., Horton, J. A., Xian, G., Auch, R. F., Sohl, T. L., Sayler, K. L., Gallant, A. L., Zelenak, D., Reker, R. R., and Rover, J.: Lessons learned implementing an operational continuous United States national land change monitoring capability: The Land Change Monitoring, Assessment, and Projection (LCMAP) approach, Remote Sens. Environ., 238, 111356, https://doi.org/10.1016/j.rse.2019.111356, 2020.

Cui, X., Kavvada, O., Huntington, T., and Scown, C. D.: Strategies for near-term scale-up of cellulosic biofuel production using sorghum and crop residues in the US, Environ. Res. Lett., 13, 124002, 2018.

Deines, J. M., Kendall, A. D., and Hyndman, D. W.: Annual Irrigation Dynamics in the U. S. Northern High Plains Derived from Landsat Satellite Data, Geophys. Res. Lett., 44, 9350–9360, https://doi.org/10.1002/2017gl074071, 2017.

Deines, J. M., Kendall, A. D., Crowley, M. A., Rapp, J., Cardille, J. A., and Hyndman, D. W.: Mapping three decades of annual irrigation across the US High Plains Aquifer using Landsat and Google Earth Engine, Remote Sens. Environ., 233, 111400, 2019.

Deines, J. M., Schipanski, M. E., Golden, B., Zipper, S. C., Nozari, S., Rottler, C., Guerrero, B., and Sharda, V.: Transitions from irrigated to dryland agriculture in the Ogallala Aquifer: Land use suitability and regional economic impacts, Agr. Water Manage., 233, 106061, https://doi.org/10.1016/j.agwat.2020.106061, 2020.

Dieter, C. A., Maupin, M. A., Caldwell, R. R., Harris, M. A., Ivahnenko, T. I., Lovelace, J. K., Barber, N. L., and Linsey, K. S.: Estimated use of water in the United States in 2015, U.S. Geological Survey, Circular 1441, 65 pp., https://doi.org/10.3133/cir1441, 2018.

Enciso, J., Jifon, J., Ribera, L., Zapata, S., and Ganjegunte, G.: Yield, water use efficiency and economic analysis of energy sorghum in South Texas, Biomass Bioenerg., 81, 339–344, 2015.

ESA: Climate Change Initiative Land Cover, http://maps.elie.ucl.ac.be/CCI/viewer/index.php (last access: 15 April 2021), 2015.

Gong, P., Li, X., Wang, J., Bai, Y., Chen, B., Hu, T., Liu, X., Xu, B., Yang, J., Zhang, W., and Zhou, Y.: Annual maps of global artificial impervious area (GAIA) between 1985 and 2018, Remote Sens. Environ., 236, 111510, https://doi.org/10.1016/j.rse.2019.111510, 2020.

Gorelick, N., Hancher, M., Dixon, M., Ilyushchenko, S., Thau, D., and Moore, R.: Google earth engine: planetary-scale geospatial analysis for everyone, Remote Sens. Environ., 202, 18–27, https://doi.org/10.1016/j.rse.2017.06.031, 2017.

Hansen, M. C., Potapov, P. V., Moore, R., Hancher, M., Turubanova, S., Tyukavina, A., Thau, D., Stehman, S., Goetz, S., and Loveland, T. R.: High-resolution global maps of 21st-century forest cover change, Science, 342, 850–853, 2013.

Jin, Y., Randerson, J. T., and Goulden, M. L.: Continental-scale net radiation and evapotranspiration estimated using MODIS satellite observations, Remote Sens. Environ., 115, 2302–2319, 2011.

Ketchum, D., Jencso, K., Maneta, M. P., Melton, F., Jones, M. O., and Huntington, J.: IrrMapper: A Machine Learning Approach for High Resolution Mapping of Irrigated Agriculture Across the Western U.S., Remote Sens., 12, 2328, https://doi.org/10.3390/rs12142328, 2020.

Lark, T. J.: Protecting our prairies: Research and policy actions for conserving America's grasslands, Land Use Policy, 97, 104727, https://doi.org/10.1016/j.landusepol.2020.104727, 2020.

Lark, T. J., Salmon, J. M., and Gibbs, H. K.: Cropland expansion outpaces agricultural and biofuel policies in the United States, Environ. Res. Lett., 10, 044003, https://doi.org/10.1088/1748-9326/10/4/044003, 2015.

Lark, T. J., Spawn, S. A., Bougie, M., and Gibbs, H. K.: Cropland expansion in the United States produces marginal yields at high costs to wildlife, Nat. Commun., 11, 4295, https://doi.org/10.1038/s41467-020-18045-z, 2020.

Lark, T. J., Schelly, I. H., and Gibbs, H. K.: Accuracy, Bias, and Improvements in Mapping Crops and Cropland across the United States Using the USDA Cropland Data Layer, Remote Sens., 13, 968, https://doi.org/10.3390/rs13050968, 2021.

Loveland, T. R., Reed, B. C., Brown, J. F., Ohlen, D. O., Zhu, Z., Yang, L., and Merchant, J. W.: Development of a global land cover characteristics database and IGBP DISCover from 1 km AVHRR data, Int. J. Remote Sens., 21, 1303–1330, 2000.

McCarthy, B., Anex, R., Wang, Y., Kendall, A. D., Anctil, A., Haacker, E. M. K., and Hyndman, D. W.: Trends in Water Use, Energy Consumption, and Carbon Emissions from Irrigation: Role of Shifting Technologies and Energy Sources, Environ. Sci. Technol., 54, 15329–15337, https://doi.org/10.1021/acs.est.0c02897, 2020.

McDonald, R. I., Green, P., Balk, D., Fekete, B. M., Revenga, C., Todd, M., and Montgomery, M.: Urban growth, climate change, and freshwater availability, P. Natl. Acad. Sci. USA, 108, 6312–6317, 2011.

Meier, J., Zabel, F., and Mauser, W.: A global approach to estimate irrigated areas – a comparison between different data and statistics, Hydrol. Earth Syst. Sci., 22, 1119–1133, https://doi.org/10.5194/hess-22-1119-2018, 2018.

Mullet, J., Morishige, D., McCormick, R., Truong, S., Hilley, J., McKinley, B., Anderson, R., Olson, S. N., and Rooney, W.: Energy Sorghum – a genetic model for the design of C4 grass bioenergy crops, J. Exp. Bot., 65, 3479–3489, 2014.

Otkin, J. A., Svoboda, M., Hunt, E. D., Ford, T. W., Anderson, M. C., Hain, C., and Basara, J. B.: Flash Droughts: A Review and Assessment of the Challenges Imposed by Rapid-Onset Droughts in the United States, B. Am. Meteorol. Soc., 99, 911–919, https://doi.org/10.1175/bams-d-17-0149.1, 2018.

Ozdogan, M. and Gutman, G.: A new methodology to map irrigated areas using multi-temporal MODIS and ancillary data: An application example in the continental US, Remote Sens. Environ., 112, 3520–3537, https://doi.org/10.1016/j.rse.2008.04.010, 2008.

Ozdogan, M., Rodell, M., Beaudoing, H. K., and Toll, D. L.: Simulating the Effects of Irrigation over the United States in a Land Surface Model Based on Satellite-Derived Agricultural Data, J. Hydrometeorol., 11, 171–184, https://doi.org/10.1175/2009jhm1116.1, 2010.

Pekel, J. F., Cottam, A., Gorelick, N., and Belward, A. S.: High-resolution mapping of global surface water and its long-term changes, Nature, 540, 418–422, https://doi.org/10.1038/nature20584, 2016.

Pervez, M. S. and Brown, J. F.: Mapping Irrigated Lands at 250 m Scale by Merging MODIS Data and National Agricultural Statistics, Remote Sens., 2, 2388–2412, https://doi.org/10.3390/rs2102388, 2010.

Pryor, S., Sullivan, R., and Wright, T.: Quantifying the roles of changing albedo, emissivity, and energy partitioning in the impact of irrigation on atmospheric heat content, J. Appl. Meteorol. Clim., 55, 1699–1706, 2016.

Robertson, G. P., Hamilton, S. K., Barham, B. L., Dale, B. E., Izaurralde, R. C., Jackson, R. D., Landis, D. A., Swinton, S. M., Thelen, K. D., and Tiedje, J. M.: Cellulosic biofuel contributions to a sustainable energy future: Choices and outcomes, Science, 356, eaal2324, https://doi.org/10.1126/science.aal2324, 2017.

Rosegrant, M. W., Ringler, C., and Zhu, T.: Water for Agriculture: Maintaining Food Security under Growing Scarcity, Annu. Rev. Env. Resour., 34, 205–222, https://doi.org/10.1146/annurev.environ.030308.090351, 2009.

Sadler, E., Evans, R., Stone, K., and Camp, C.: Opportunities for conservation with precision irrigation, J. Soil Water Conserv., 60, 371–378, 2005.

Salmon, J. M., Friedl, M. A., Frolking, S., Wisser, D., and Douglas, E. M.: Global rain-fed, irrigated, and paddy croplands: A new high resolution map derived from remote sensing, crop inventories and climate data, Int. J. Appl. Earth Obs., 38, 321–334, https://doi.org/10.1016/j.jag.2015.01.014, 2015.

Sanderson, M. A., Jolley, L. W., and Dobrowolski, J. P.: Pastureland and hayland in the USA: Land resources, conservation practices, and ecosystem services, Conservation outcomes from pastureland and hayland practices: Assessment, recommendations, and knowledge gaps, Allen Press, Lawrence, KS, 25–40, 2012.

Seager, R., Ting, M., Li, C., Naik, N., Cook, B., Nakamura, J., and Liu, H.: Projections of declining surface-water availability for the southwestern United States, Nat. Clim. Change, 3, 482–486, https://doi.org/10.1038/nclimate1787, 2012.

Senay, G. B., Friedrichs, M., Singh, R. K., and Velpuri, N. M.: Evaluating Landsat 8 evapotranspiration for water use mapping in the Colorado River Basin, Remote Sens. Environ., 185, 171–185, 2016.

Senay, G. B., Schauer, M., Friedrichs, M., Velpuri, N. M., and Singh, R. K.: Satellite-based water use dynamics using historical Landsat data (1984–2014) in the southwestern United States, Remote Sens. Environ., 202, 98–112, 2017.

Seto, K. C., Guneralp, B., and Hutyra, L. R.: Global forecasts of urban expansion to 2030 and direct impacts on biodiversity and carbon pools, P. Natl. Acad. Sci. USA, 109, 16083–16088, https://doi.org/10.1073/pnas.1211658109, 2012.

Seyoum, W. M. and Milewski, A. M.: Monitoring and comparison of terrestrial water storage changes in the northern high plains using GRACE and in-situ based integrated hydrologic model estimates, Adv. Water Resour., 94, 31–44, 2016.

Shrestha, D., Brown, J. F., Benedict, T. D., and Howard, D. M.: Exploring the Regional Dynamics of U. S. Irrigated Agriculture from 2002 to 2017, Land, 10, 394, https://doi.org/10.3390/land10040394, 2021.

Siebert, S., Döll, P., Hoogeveen, J., Faures, J.-M., Frenken, K., and Feick, S.: Development and validation of the global map of irrigation areas, Hydrol. Earth Syst. Sci., 9, 535–547, https://doi.org/10.5194/hess-9-535-2005, 2005.

Siebert, S., Henrich, V., Frenken, K., and Burke, J.: Global map of irrigation areas version 5, Rheinische Friedrich-Wilhelms-University, Bonn, Germany/Food and Agriculture Organization of the United Nations, Rome, Italy, 2013.

Teluguntla, P. G., Thenkabail, P. S., Xiong, J., Gumma, M. K., Giri, C., Milesi, C., Ozdogan, M., Congalton, R., Tilton, J., and Sankey, T. T.: Global Cropland Area Database (GCAD) derived from remote sensing in support of food security in the Twenty-First Century: Current achievements and future possibilities, Taylor & Francis, Boca Raton, Florida, USA, 2015.

Thenkabail, P. S., Biradar, C. M., Noojipady, P., Dheeravath, V., Li, Y., Velpuri, M., Gumma, M., Gangalakunta, O. R. P., Turral, H., and Cai, X.: Global irrigated area map (GIAM), derived from remote sensing, for the end of the last millennium, Int. J. Remote Sens., 30, 3679–3733, 2009.

Troy, T. J., Kipgen, C., and Pal, I.: The impact of climate extremes and irrigation on US crop yields, Environ. Res. Lett., 10, 054013, https://doi.org/10.1088/1748-9326/10/5/054013, 2015.

Turral, H., Svendsen, M., and Faures, J. M.: Investing in irrigation: Reviewing the past and looking to the future, Agr. Water Manage., 97, 551–560, 2010.

USDA: https://www.ers.usda.gov/topics/farm-practices-management/irrigation-water-use/background/, last access: 15 June 2021.

USDA-NASS: 2017 Census of Agriculture, Summary and State Data, Geographic Area Series, Part 51, AC-17–A-51, US Department of Agriculture, Washington D.C., USA, 2019.

USDA-NASS: https://www.usda.gov/media/blog/2021/02/11/usda-invests-data-agricultural-irrigation-improvements, last access: 15 June 2021.

USGS: National Water Census, available at: https://www.usgs.gov/mission-areas/water-resources/science/national-water-census-water-use (last access: 15 June 2021), 2020a.

USGS: USGS Water Use Data for the Nation, available at: https://waterdata.usgs.gov/nwis/wu (last access: 15 June 2021), 2020b

USGS: Water Availability and Use Science Program, available at: https://www.usgs.gov/water-resources/water-availability-and-use-science-program (last access: 15 June 2021), 2020c.

van Vliet, J.: Direct and indirect loss of natural area from urban expansion, Nature Sustainability, 2, 755–763, https://doi.org/10.1038/s41893-019-0340-0, 2019.

Wardlow, B. D. and Callahan, K.: A multi-scale accuracy assessment of the MODIS irrigated agriculture data-set (MIrAD) for the state of Nebraska, USA, GISci. Remote Sens., 51, 575–592, 2014.

Wickham, J., Stehman, S. V., Sorenson, D. G., Gass, L., and Dewitz, J. A.: Thematic accuracy assessment of the NLCD 2016 land cover for the conterminous United States, Remote Sens. Environ., 257, 112357, https://doi.org/10.1016/j.rse.2021.112357, 2021.

Xie, Y. and Lark, T. J.: LANID-US: Landsat-based Irrigation Dataset for the United States, Zenodo [data set], https://doi.org/10.5281/zenodo.5548555, 2021a.

Xie, Y. and Lark, T. J.: Mapping annual irrigation from Landsat imagery and environmental variables across the conterminous United States, Remote Sens. Environ., 260, 1–17, https://doi.org/10.1016/j.rse.2021.112445, 2021b.

Xie, Y., Weng, Q., and Fu, P.: Temporal variations of artificial nighttime lights and their implications for urbanization in the conterminous United States, 2013–2017, Remote Sens. Environ., 225, 160–174, https://doi.org/10.1016/j.rse.2019.03.008, 2019a.

Xie, Y., Lark, T. J., Brown, J. F., and Gibbs, H. K.: Mapping irrigated cropland extent across the conterminous United States at 30 m resolution using a semi-automatic training approach on Google Earth Engine, ISPRS J. Photogramm., 155, 136–149, https://doi.org/10.1016/j.isprsjprs.2019.07.005, 2019b.

Xu, T., Deines, J., Kendall, A., Basso, B., and Hyndman, D.: Addressing Challenges for Mapping Irrigated Fields in Subhumid Temperate Regions by Integrating Remote Sensing and Hydroclimatic Data, Remote Sens., 11, 370, https://doi.org/10.3390/rs11030370, 2019.

Yin, H., Brandão, A., Buchner, J., Helmers, D., Iuliano, B. G., Kimambo, N. E., Lewińska, K. E., Razenkova, E., Rizayeva, A., Rogova, N., Spawn, S. A., Xie, Y., and Radeloff, V. C.: Monitoring cropland abandonment with Landsat time series, Remote Sens. Environ., 246, 111873, https://doi.org/10.1016/j.rse.2020.111873, 2020.

Zaussinger, F., Dorigo, W., Gruber, A., Tarpanelli, A., Filippucci, P., and Brocca, L.: Estimating irrigation water use over the contiguous United States by combining satellite and reanalysis soil moisture data, Hydrol. Earth Syst. Sci., 23, 897–923, https://doi.org/10.5194/hess-23-897-2019, 2019.